

Cosmogenic neutrinos as probes of new physics

Luighi P. S. Leal^{1*}, Daniel Naredo-Tuero^{2†}, Renata Zukanovich Funchal^{1‡}

¹Instituto de Física, Universidade de São Paulo, C.P. 66.318, 05315-970 São Paulo, Brazil

²Departamento de Física Teórica and Instituto de Física Teórica UAM/CSIC,
Universidad Autónoma de Madrid, Cantoblanco, 28049 Madrid, Spain

Abstract

The scattering of extremely energetic cosmic rays with both cosmic microwave background and extragalactic background light, can produce $\mathcal{O}(10^{18}$ eV) neutrinos, known as cosmogenic neutrinos. These neutrinos are the only messengers from the extreme cosmic accelerators that can reveal the origin of the most energetic cosmic rays. Consequently, much effort is being devoted to achieving their detection. In particular, the GRAND project aims to observe the ν_τ and $\bar{\nu}_\tau$ components of the cosmogenic neutrino flux in the near future using radio antennas. In this work, we investigate how the detection of cosmogenic neutrinos by GRAND can be used to probe beyond the Standard Model physics. We identify three well-motivated scenarios which induce distinct features in the cosmogenic neutrino spectrum at Earth: neutrino self-interactions mediated by a light scalar (ν SI), pseudo-Dirac neutrinos (PD ν) and neutrinos scattering on ultra-light Dark Matter (ν DM). We show these scenarios can be tested by GRAND, using 10 years of cosmogenic neutrino data, in a region of parameter space complementary to current experiments. For the ν SI model, we find that GRAND can constrain the coupling to ν_τ in the range $[10^{-2}, 10^{-1}]$ for a scalar with mass in the range 0.1 to 1 GeV. For PD ν , we find that GRAND is sensitive to sterile-active mass squared splitting in the range $[10^{-15}, 10^{-13}]$ eV². Finally, for the ν DM model, assuming a heavy mediator, GRAND can do substantially better than the current limits from other available data. These results rely on the fact that the actual cosmogenic flux is around the corner, not far from the current IceCube limit.

*luighi.leal@usp.br

†daniel.naredo@ift.csic.es

‡zukanov@if.usp.br

Contents

1	Introduction	1
2	Modeling of the Cosmogenic Neutrino Flux	3
3	Modeling of the Radio Array Detector Response	5
4	BSM Scenarios	7
4.1	Neutrino self-interactions (ν SI)	7
4.2	Pseudo-Dirac neutrinos ($PD\nu$)	10
4.3	Neutrinos Scattering on Ultra-light Scalar Dark Matter (ν DM)	13
5	Analysis and Results	16
6	Final Conclusions	22
A	On the propagation of Cosmic Rays	25
B	Neutrino-Ultralight Dark Matter Cross Section	26

1 Introduction

Cosmic rays, since their discovery by Victor Hess in 1912, have been connected to advances in our understanding of nature. It was in the study of cosmic rays that in the first half of the last century we observed the positron, the muon and the pion for the first time. In 1998 neutrino flavor oscillations were first demonstrated by observing the flavor composition of atmospheric neutrinos that arrived at the Earth and were produced by cosmic rays [1]. Since 2013 the IceCube Neutrino Observatory is detecting an unexpected flux of very high-energy neutrinos (in the hundreds of TeV to tens of PeV range) of extragalactic origin [2]. If this neutrino flux is related or not to the sources of high-energy cosmic rays is still an open question. The characterization of the neutrino spectrum and flavor composition beyond the current energy range attainable by IceCube will be crucial in resolving the sources. This may also provide new ways to probe the most extreme particle accelerators in our Universe.

These cosmic accelerators remain hidden ultimately because the Universe becomes opaque at scales ~ 100 Mpc for extreme energy cosmic rays (EECRs), with energies $\gtrsim 50$ EeV. This is because, at those energies, the scattering of EECRs with photons of the cosmic microwave background (CMB) and of the extragalactic background light (EBL) triggers the Δ^+ resonance [3–5]. As a by-product of these resonant scatterings, the so-called cosmogenic neutrinos are produced mainly through pion or neutron decays. Unstable nuclei, which result from photodisintegration or photo-pion production, can also suffer beta decay further adding to this cosmogenic neutrino flux [6]. Cosmogenic neutrinos can then carry information from cosmic accelerators located at much larger distances from Earth than the ones we can inspect with EECRs. Moreover, cosmogenic neutrinos are expected to have energies of about 10^{18} eV (1 EeV) and to be viable probes of the sources of EECRs since their imperviousness to magnetic fields and extremely low interaction rate imply that they arrive at Earth only modified by energy redshift and flavor oscillation.

Although the existence of cosmogenic neutrinos is basically guaranteed ¹, the theoretical prediction of the expected diffuse flux, however, is plagued by astrophysical uncertainties concerning the primary source properties. When modeling this flux, assumptions have to be made about ingredients such as the chemical composition, the injected spectral index, the luminosity, the maximal energy attainable, and the cosmological evolution. The diffuse flux may also be the result of a homogeneous distribution of identical sources or of a mixture of different types of sources. Fortunately, these astrophysical uncertainties seem to mainly affect the overall normalization of the flux, which typically spans several orders of magnitude but has the same general spectral shape predicted by different astrophysical models [6, 8–10].

On the other hand, cosmogenic neutrinos may turn out to be invaluable not only for the investigations of these extreme astronomical sources, but also for probing neutrino properties [10–12] and testing specific Beyond the Standard Model (BSM) scenarios [13–17].

There are a few next generation projects aiming to provide sensitivity for neutrinos with energy $E_\nu \sim 1$ EeV at an energy flux level $E_\nu^2 \Phi_\nu \lesssim 10^{-9}$ GeV cm⁻² s⁻¹ sr⁻¹ exploring radio detection techniques currently developed by experiments such as ANITA [18], ARA [19] and ARIANNA [20] to measure radio pulses generated by charged particle cascades (Askaryan emission) induced by neutrino interactions in matter. The most promising are the Giant Radio Array for Neutrino Detection (GRAND) [21] and the IceCube-Gen2 radio array [22] ² The GRAND antennas are designed to detect inclined extensive air-shower (EAS) ³. This makes them mainly sensitive to tau neutrinos (ν_τ). Cosmogenic ν_τ 's can produce EAS emerging from the Earth (rock or ice) if they interact producing a τ lepton close enough to the Earth's surface. Typically, at the expected energies, the τ lepton can travel a few tens of km in matter before exiting in the atmosphere and decaying, thus generating an Earth-skimming EAS.

There are two caveats we would like to point out here. First, neutrino-nucleon SM cross section predictions are accurate only up to 10^{-1} EeV mainly due to limitations of extrapolating parton distribution functions at lower Bjorken- x than currently accessible by colliders and fixed target accelerator experiments [25–27]. Second, the effect of final state radiation (FSR) has to be accounted for. It seems that if FSR is not included in the calculation it will lead to the underestimation of the parent neutrino energy by about 5% (smaller than the energy resolution of GRAND). But FSR also affects the regeneration process as it lowers the tau energy [28]. The first problem can be solved in the future by means of experimental data at higher energies and possible improvements of theoretical techniques. The second can be solved by incorporating FSR in the calculations. We estimate that together they can affect our results by 10-20%.

The purpose of this paper is to assess the use of these future radio arrays in investigating BSM physics that can produce distinct features in the observable cosmogenic neutrino spectrum (such as dips or bumps) that can be disentangled from the astrophysical uncertainties in the normalization and shape of the standard flux. We start in section 2 by describing how we model and simulate the cosmogenic neutrino flux. In section 3 we describe how we model the GRAND radio array detector response to Earth-skimming ν_τ . Section 4 is devoted to presenting the three BSM scenarios we will study here: neutrino self-interactions, pseudo-

¹The first neutrino event observed by KM3NeT, KM3-230213A [7], may be of cosmogenic origin.

²There is also the Probe Of Extreme Multi-Messenger Astrophysics (POEMMA) [23] which is a NASA Astrophysics probe-class mission to identify cosmogenic tau neutrinos above 20 PeV.

³IceCube-Gen2, on the other hand, relies on detecting the radio waves from scatterings of neutrinos *inside* the ice. Since they don't require the charged lepton to exit the Earth and produce a EAS, IceCube-Gen2 is approximately sensitive to all flavors. See, for example, Section 4 of Ref. [24].

Dirac neutrinos, and neutrinos scattering on ultra-light scalar Dark Matter. In section 5 we introduce our analysis and examine our results. We draw our conclusions and give our final remarks in section 6. We also provide two appendices; in A we review the main ingredients behind the calculation of the cosmogenic neutrino flux at the Earth and in B we give the expression for the neutrino-ultralight Dark Matter differential cross section.

2 Modeling of the Cosmogenic Neutrino Flux

The EECRs spectrum and chemical composition is highly unknown, and there seems to be some incompatibility between different experiments. While Auger seems to disfavor a sizeable light component between 50 - 100 EeV [29], the Telescope Array collaboration reports compatibility with a moderately light composition below 100 EeV [30]. These data have been used to make predictions about the diffuse cosmogenic neutrino flux [6, 31, 32]. In fact, global fits to the source composition of these EECR sources seem to disfavor a pure-proton composition [29, 33]. However, the existence of a proton (or light nuclei) subdominant or even dominant component at the highest energies cannot be ruled out by data [30, 34, 35]. If the recent KM3NeT ~ 0.1 EeV event [7] is indeed of cosmogenic origin, this may indicate a non-negligible proton component at those energies. In fact, cosmic-ray observations on Earth are dominated by sources at $\lesssim 300$ Mpc and sources located beyond this distance could have a different behavior [31]. This component could be produced by a secondary population of sources that could exclusively accelerate protons to extreme energies or where heavier nuclei are disintegrated before escaping the source region. This would have a limited effect on the full ultra-high-energy cosmic ray spectrum. Even a subdominant proton or light nuclei component would alter the expected cosmogenic neutrino flux since they produce significantly more neutrinos than heavier nuclei.

For the modeling and simulation of the sources of EECRs and the production of cosmogenic neutrinos, we closely follow Refs. [36, 37]. In Appendix A we give a brief description of the type of integro-differential equations one needs to solve to compute the flux $\Phi_\nu(E_\nu)$ at the Earth. For the sake of simplicity, we will assume here pure-proton sources with a power-law injection spectrum

$$\frac{dN_p}{dE_p} \propto E_p^{-\gamma} \exp\left(-\frac{E_p}{E_{\max}}\right), \quad (1)$$

with the spectral index γ and the proton energy E_p varying in the range from 10 EeV to E_{\max} .

The assumption of pure-proton sources might seem too optimistic given the constraints on the mass composition of EECRs. However, it has been shown that the source composition is degenerate with the redshift evolution of the sources [36, 37] since, for a fixed spectral index, both modify the normalization of the flux. Moreover, this is not the most optimistic case in terms of cosmogenic neutrino production, as intermediate nuclei, such as He and N, can lead to larger fluxes (see, for example, Appendix A of [36]).

In our scenario we consider a distribution of identical proton sources with the same luminosity which extend up to redshift $z_{\max} = 7$. We parametrise the source evolution as

$$\text{SE}(z, m) = \begin{cases} (1+z)^m & z < 1, \\ 2^m & 1 \leq z < 4, \\ 2^m \left(\frac{1+z}{5}\right)^{-3.5} & 4 \leq z < 7, \end{cases} \quad (2)$$

where the choice $m = 3$ for the source evolution parameter would correspond to a redshift evolution similar to the star formation rate [38], while $m = 0$ would mimic the typical redshift evolution of BL-Lac models [39, 40]. The range of m depends on the class of the sources [36, 37]. So this parametrization allows us to approximate the redshift evolution of different classes of sources.

We simulate the propagation and scattering of the EECR protons with the CRPropa3 code [41]. This code includes all relevant interactions for the calculation of the cosmogenic flux (photo-pion production, pair production, nuclear β decay) and adiabatic energy losses due to the expansion of the Universe.

We perform an extragalactic 1D simulation (i.e. neglecting magnetic fields) keeping track of both protons and neutrinos. Magnetic-field effects are expected to increase the cosmogenic neutrino flux by a factor of a few at $E_\nu \sim 1$ EeV [42]. The photon fields against which the EECR protons will scatter are the CMB and the EBL, and we use the EBL model from Ref. [43]. According to Ref. [44] the choice of the EBL model has a minor effect as the CMB is the dominant photon field for neutrino production in the energy range of interest.

In the free-streaming case, the neutrino flux is simply

$$\Phi_\nu(E_\nu) = \frac{1}{4\pi} \int_0^{z_{\max}} dz \frac{\mathcal{L}_\nu(z, (z+1)E_\nu)}{H(z)}, \quad (3)$$

where $\mathcal{L}_\nu(z, E) = \text{SE}(z, m) \mathcal{L}_\nu(0, E)$ and $\mathcal{L}_\nu(0, E) \propto dN_p/dE_p$.

As a means of normalising the total flux, we make use of the EECR spectrum in the energy range 40-100 EeV, as measured by the Pierre Auger Observatory [45, 46]. Specifically, as in Ref. [44], the normalisation is chosen to match the measured EECR spectrum at $E_0 = 10^{19.55}$ eV. Since EECRs can only travel distances of the order of ~ 100 Mpc before scattering, the measurement from Auger comes from very low redshift and thus the normalisation can be considered almost independent of the source evolution.

All in all, in our simplified modeling setup, the injected cosmogenic neutrino flux is given in terms of only three parameters: the spectral index of the injected proton spectrum (γ), the maximum value of the proton energy (E_{\max}) and the source evolution parameter (m).

In Fig. 1 we show the simulated cosmogenic neutrino spectra⁴ at the Earth for different values of the spectral index $\gamma = 2$ and 3 (top-left panel), of the maximum energy $E_{\max} = 10^2$ EeV and 10^5 EeV (top-right panel) and of the evolution parameter $m = 0$ and 3 (bottom-left panel). We are assuming the flavor ratio at the Earth to be $\nu_e : \nu_\mu : \nu_\tau = 1 : 1 : 1$ in accordance with what is expected from standard neutrino oscillation experimental results [47] when the dominant neutrino production is π -decay. The parameters that are not varied are kept in their value of the benchmark point: $\gamma = 2.5$, $E_{\max} = 250$ EeV and $m = 3$. To illustrate the fact our parametrisation of the source evolution can mimic different chemical compositions, because of the degeneracy with m , we show in the bottom-right panel of Fig. 1 the simulated cosmogenic spectrum considering the source to produce, besides protons, a certain fraction α_S of iron.

From this figure we can appreciate the effect of each astrophysical parameter on the spectrum, giving an indication of how our BSM results will depend on our assumptions on their values. A lower (higher) spectral index shifts the peak of the spectrum to higher (lower) energies. Clearly, a lower (higher) E_{\max} will produce a lower (higher) cut-off, decreasing (increasing) the

⁴The cosmogenic neutrino spectra we will present throughout this paper will always be the single-flavor one, i.e., ν_τ and $\bar{\nu}_\tau$ spectra combined.

cosmogenic flux at higher energies. Note also that in the range $2 \times 10^8 \lesssim E_\nu/\text{GeV} \lesssim 2 \times 10^9$ the neutrino spectrum is almost not affected by the choice of γ or E_{max} , this behavior does not depend on m . The source evolution parameter (or the chemical composition) is the main responsible for the overall normalization, $m = 3$ is a typical value for the star formation rate while $m = 0$, flat evolution, is allowed by some tidal disruption event and BL Lac models [37].

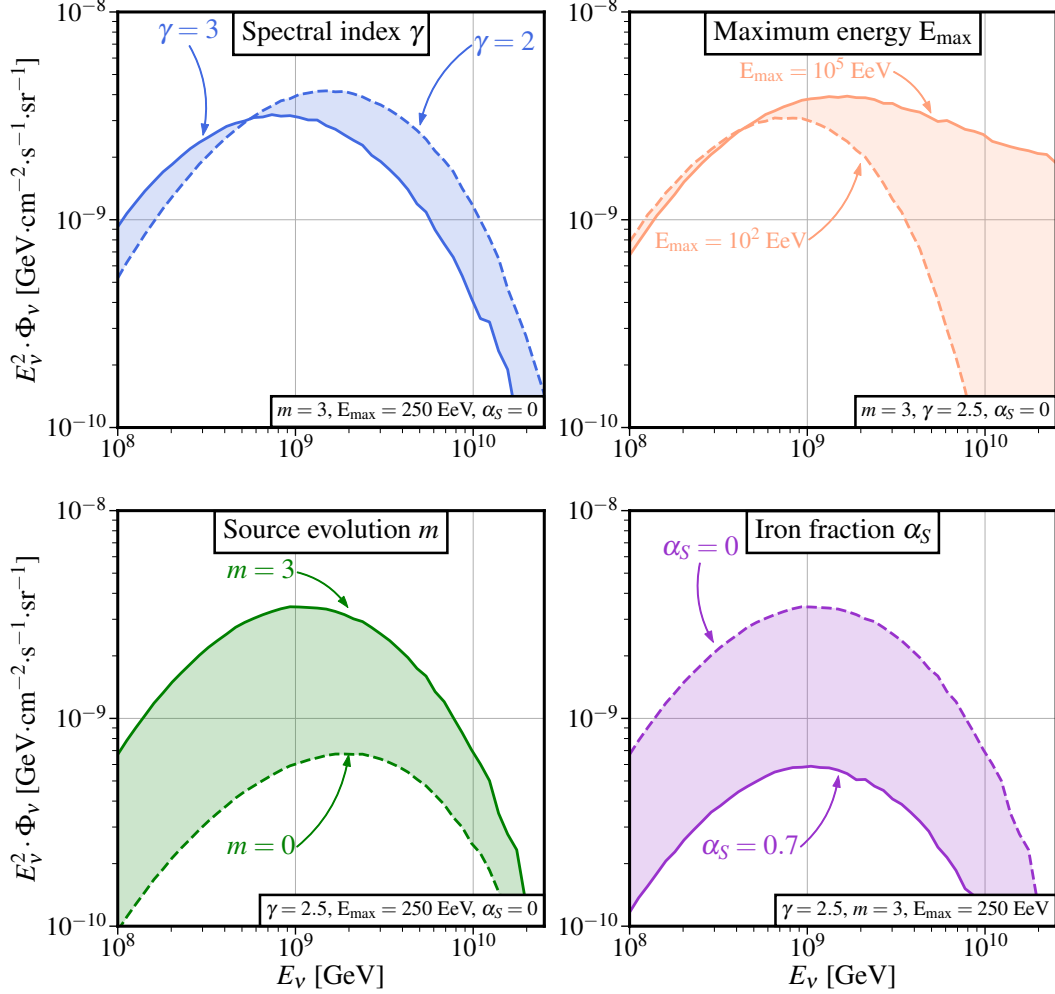


Figure 1: Simulated single-flavor cosmogenic neutrino spectra assuming the flavor ratio at the Earth to be $\nu_e : \nu_\mu : \nu_\tau = 1 : 1 : 1$, for different values of the spectral index γ , maximum energy E_{max} , source evolution parameter m , and in the last panel, besides protons, we consider a fraction α_S of iron. Except for the last panel (bottom-right) all cases are for a pure-proton scenario.

3 Modeling of the Radio Array Detector Response

We will consider the GRAND project [21], which aims to extend the field of radio-detection of EAS to include events initiated by Earth-skimming neutrinos, as the prototype for a radio array of antennas. This will allow us to access the sensitivity of this type of detector to BSM

physics that can affect the cosmogenic neutrino flux in a distinctive way.

In principle, at EeV energies the Earth is opaque even to Earth-skimming neutrinos. At those energies the neutrino-nucleon deep-inelastic scattering cross section increases as $E^{0.363}$ [48] so the neutrino interaction length inside the Earth will be only of a few hundred kilometers. If the neutrino interacts via charged current, it will produce a charged lepton of the same flavor of the incoming neutrino. For ν_e , the outgoing electron will give rise to a short-lived electromagnetic shower concentrated around the point of interaction. Even if this shower starts close to the surface, the maximum column depth that the shower can traverse is about 30-40 m underground, making the expected effective volume for radio detection too small. For ν_μ , the outgoing high energy μ can travel from the point of creation in the rock to the atmosphere where it will have a range of several kilometers. The probability that this μ will decay above the radio array generating a detectable EAS seems also to be negligible. For ν_τ , however, things are different because of the properties of the τ lepton. First, it is the heaviest charged lepton so radiative losses are the most suppressed. Second, it has a short lifetime ($\tau_\tau \sim 2.9 \times 10^{-13}$ s) which implies a range $\gamma c \tau_\tau \sim 50$ km ($E_\tau/1$ EeV) before decaying. Third, since the decay of a τ also produces a ν_τ , the attenuation of the neutrino flux due to interaction as it propagates in matter is compensated by ν_τ regeneration⁵. So a τ produced by a ν_τ underground can exit the Earth and decay in-flight in the atmosphere above the radio array triggering a detectable EAS. As the EAS develops in the atmosphere, the geomagnetic field separates positive from negative charges creating a time-dependent electric current which induces radio emission. Due to Compton scattering, an excess of negative charge builds up in the EAS during propagation also inducing radio emission. This is known as the Askaryan effect [49, 50]. In dense media, like ice, the Askaryan effect is more important, while in air the geomagnetic effect dominates. Both emissions are coherent and beamed in the forward direction, inside a narrow cone of half-width equal to the Cherenkov angle.

Furthermore, most of the τ decays are into hadrons (65%) or electrons (20%) so once the τ reaches the atmosphere, the probability of creating a detectable air shower is rather high, i.e. only the τ decays into muons will not emit a significant radio signal (as in the case of ν_μ).

The idea is to instrument a large area using a sparse array. The strategy is to divide GRAND into 10 to 20 geographically separate and favorable to neutrino detection independent sub-arrays, each containing about 10^4 antennas. Ideally, the antenna array should be deployed on a mountain slope facing another mountain that could serve as an additional target for interaction. This mountain should be distant enough (few tens of km) for the EAS to develop and the radio cone to become large enough before hitting the antennas.

GRAND is expected to have a very good (sub-degree) angular resolution. This can, among other things, help to reject background events coming from above the horizon. Preliminary estimates indicate that one expects less than 0.1 per year ultra-high-energy cosmic ray misidentified as a neutrino in GRAND200k, a combined area of 200 000 km², with the angular aperture $85^\circ \leq \theta \leq 95^\circ$ [21].

It should also be mentioned that not all cosmogenic neutrino observatories will have the same detection techniques. For instance, the IceCube-Gen2 radio array [22, 24] will be embedded in the ice; therefore, it will be sensitive to interactions of cosmogenic neutrinos of any flavor. In fact, the different flavor sensitivity of these observatories may be harnessed to constrain the production mechanisms of cosmogenic neutrinos [51].

In order to convert the calculated cosmogenic neutrino energy spectrum into the number

⁵This may shift the flux to lower energies as the regenerated ν_τ receives $\sim 30\%$ of the parent τ energy.

of ν_τ events detected at GRAND, one needs to know the effective area of the array. The GRAND collaboration has already simulated the effective area of *HotSpot 1* (HS1), a 10 000 km² area located at the Southern rim of the Tian Shan mountain range in China, thus having an exceptionally good exposure to neutrinos. We will make use of the direction-averaged effective area shown in Fig. 25 of [21] as a GRAND200k⁶ estimation, obtained by multiplying by 20 the HS1 effective area with an aggressive energy threshold for the radio antennas⁷. On the left panel of Fig. 2 we show the effective area we use in this work.

The energy resolution of the reconstructed EAS is expected to be of 15%. However, it is initiated by a τ which carries an unknown fraction of the energy of the parent ν_τ . So to estimate the neutrino energy resolution, one first needs to reconstruct the energy of the shower and then unfold into the neutrino energy, taking into account the fraction of energy carried by the τ as well as the energy losses of ν_τ and τ in matter. It seems plausible to assume an neutrino energy resolution of $\Delta \log_{10} E_\nu = 0.25$, as proposed in [36]. In our simplified detector simulation, we will estimate the number of ν_τ events at GRAND by smearing the cosmogenic ν_τ spectrum, calculated according to each BSM scenario (see section 4), times the effective area with a log-normal distribution adopting this energy resolution as the width. We will collect the number of events in 9 log-energy bins of width $\Delta \log_{10} E_\nu = 0.25$, from $E_\nu = 10^{17}$ eV to $E_\nu = 10^{19.25}$ eV. On the right panel of Fig. 2 we illustrate the effect of the energy resolution on the distribution of cosmogenic neutrino events. In particular, we have artificially added a dip of width $\Delta \log_{10} E_\nu = 0.25$ at $E_\nu = 0.7$ EeV to mock a spectrum which mimics the typical signature of some of the BSM scenarios that will be studied. The plot highlights the relevance of including the energy resolution, as it tends to smooth out any spectral feature, thus significantly reducing the sensitivity.

4 BSM Scenarios

We have identified a few interesting BSM scenarios which can modify the expected cosmogenic ν_τ energy spectrum at GRAND in a distinct observable way, which cannot be imitated by a simple renormalization of the distribution.

4.1 Neutrino self-interactions (ν SI)

Secret neutrino-neutrino interactions [52] can significantly alter the propagation of cosmogenic neutrinos, as they can induce scattering with relic neutrinos from the Cosmic Neutrino Background (C ν B) radiation leaving visible imprints on the cosmogenic ν_τ spectrum [53], as the baselines traveled by these neutrinos are very large. We focus on the scalar interaction case, as it is the least constrained setup today. As such, we consider the following Lagrangian to describe these interactions with Majorana neutrinos⁸

⁶The ultimate goal of GRAND is to have 20 similar setups.

⁷In this case the antennas are triggered if the peak-to-peak amplitude of the voltage signal exceeds 30 μ V, instead of the conservative threshold of 75 μ V, increasing the effective area by a factor of 2.5 with respect to the conservative case. This also gives twice the expected background noise in the 50-200 MHz frequency range of the antennas.

⁸We use this effective Lagrangian description which is enough for our study. Possible gauge invariant UV complete models that can give rise to this can be found, for instance, in [54–56]. Note that ϕ can only couple to the SM fields via dimension six or higher operators [57].

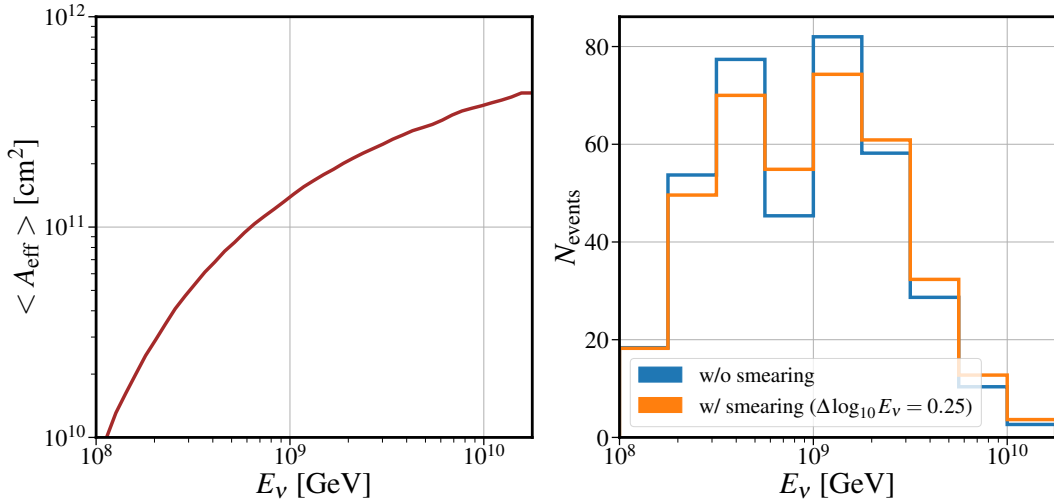


Figure 2: Direction-averaged effective area (left panel) and effect of the energy resolution in the distribution of events (right panel). The effective area has been taken from Ref. [21], while for the energy resolution we demonstrate its effect by means of a mock flux in which a spectral feature (a dip) has been artificially added so as to mimic the possible signatures of the BSM models under consideration.

$$-\mathcal{L} \supset \frac{1}{2} g_\phi^{\alpha\beta} \overline{\nu_{\alpha L}} \nu_{\beta L}^c \phi + \text{h.c.} + \frac{1}{2} m_\phi^2 \phi^2, \quad (4)$$

where ϕ is the real scalar mediator with mass m_ϕ and we denote the flavor indices as $\alpha, \beta = e, \mu, \tau$. Note that, at the energies we are interested in, scalar and pseudoscalar interactions give the same results. This scalar mediator is a SM singlet and carries a $+2$ ($B - L$) charge. Since relic neutrinos are non-relativistic, the center-of-mass energy of the scattering of a cosmogenic neutrino of energy E_ν and a relic neutrino will be given by $s = 2E_\nu m_i$, where $m_i \lesssim 0.1$ eV is the neutrino mass. When the condition

$$s = 2E_\nu m_i = m_\phi^2, \quad (5)$$

is met, the cross section is resonantly enhanced and can lead to a dip in the spectrum of cosmogenic neutrinos with energies satisfying the above condition, as the Universe becomes opaque to those neutrinos. We will always assume that all neutrino mass eigenvalues are larger than the temperature of the C ν B so that all cosmic neutrinos can be considered non-relativistic in the redshift interval of interest. For the sake of simplicity, we will assume Normal Ordering and a value of $\sum m_i = 0.1$ eV, although results for a different $\sum m_i$ will be qualitatively similar, as long as all $m_{\text{lightest}} \gg T_{\text{C}\nu\text{B}}$. It should be noted that, if the lightest neutrino mass eigenstate lies below $T_{\text{C}\nu\text{B}} \simeq 1.7 \cdot 10^{-4}$ eV, its Fermi-Dirac distribution would allow for a broadening of the neutrino absorption feature, thus increasing the sensitivity to νSI [58].

Therefore, provided that GRAND is able to measure a sufficient number of ν_τ events in order to reconstruct their energy spectrum, it should have sensitivity for mediators whose masses can satisfy the resonance condition, i.e. $100 \text{ MeV} \lesssim m_\phi \lesssim 1 \text{ GeV}$, for E_ν in the range 0.1 to 10 EeV.

For the sake of simplicity, we will restrict ourselves to a mediator that couples predominantly to tau neutrinos, i.e. $g_\phi^{\alpha\beta} = g_{\tau\tau} \delta_{\alpha\tau} \delta_{\beta\tau}$. This approach is also justified because ν_τ

self-interactions are the least explored as the scalar coupling to electron and muon neutrinos are significantly more constrained in the m_ϕ range we are exploring here. Furthermore, the authors of Ref. [59] pointed out that neutrino self interaction can explain the tension in the Hubble parameter if $m_\phi \sim 10$ MeV and has large couplings (almost) exclusively to ν_τ . In this simplified setup, our ν SI model is described by only two parameters: the mediator mass, m_ϕ , and its coupling to ν_τ , $g_{\tau\tau}$.

On their way to Earth, cosmogenic ν_τ and $\bar{\nu}_\tau$ may scatter with the C ν B due to ν SI. As a consequence, higher-energy neutrinos are absorbed and lower-energy neutrinos are re-generated. One can estimate the size of the cross section $\sigma_{\nu\text{SI}}$ which can significantly affect propagation by requiring that the optical depth for this interaction as

$$\tau_\nu \simeq \frac{n_{\text{C}\nu\text{B}} \sigma_{\nu\text{SI}}}{h_0} = 1,$$

where $h_0 = 67.3 \text{ km s}^{-1} \text{ Mpc}^{-1}$ is the Hubble parameter (we consider h_0^{-1} as the typical traveled distance scale from the astrophysical source⁹) and $n_{\text{C}\nu\text{B}} \sim 56 \text{ cm}^{-3}$ [60] is the target C ν B number density for ν_τ (or $\bar{\nu}_\tau$). This results in a cross section $\sigma_{\nu\text{SI}} \sim 10^{-30} \text{ cm}^2$, much higher than $\sigma_{\nu\text{SM}} \simeq G_{\text{F}}^2 s \sim 10^{-37} \times (E_\nu/\text{EeV}) \times (m_\nu/\text{eV}) \text{ cm}^2$ expected for SM neutrino-neutrino scattering.

In order to estimate how ν SI modifies the cosmogenic neutrino flux, we will make use of the code `nuSIprop` [61], which solves the transport equation of high-energy neutrinos (see Eq. (24)) in the presence of self interactions. In this case the interaction terms to be included in the transport equation [62, 63] are

$$\Gamma_\nu(z, E(z, E_\nu)) = n_{\text{C}\nu\text{B}}(z) \sigma_{\nu\text{SI}}(E(z, E_\nu)), \quad (6)$$

and

$$\int dE' \frac{\sigma_{ji}}{dE} \rightarrow n_{\text{C}\nu\text{B}}(z) \int_0^\infty dE'_\nu \frac{d\sigma_{\nu\text{SI}}}{dE'_\nu}(E_\nu, E'_\nu), \quad (7)$$

where $\sigma_{\nu\text{SI}}$ is the $\nu\nu \rightarrow \nu\nu$ scattering cross-section that can be found in Appendix A of Ref. [61].

Since `nuSIprop` considers a power-law injection spectrum for the neutrinos, which is not valid for cosmogenic neutrinos, we have adapted the code to take into account the cosmogenic spectral shape and its redshift dependence. For this purpose, we simulate the cosmogenic neutrino spectrum with `CRPropa3` as described in the previous section, and then we interpolate its shape both in energy and redshift. This interpolated spectrum is then fed into `nuSIprop`, which propagates the neutrinos taking ν SI into account.

For a given point of the parameter space ($m_\phi, g_{\tau\tau}, \gamma, m, E_{\text{max}}$) we compute the modified cosmogenic neutrino flux arriving at the Earth. In Fig. 3 we illustrate the effect of ν SI in the neutrino flux (left panel) as well as the observed number of events (right panel). The double dip feature shown in the right panel corresponds to the energies in which the resonance condition $2E_\nu m_i = m_\phi^2$ is met. Since we have assumed Normal Ordering, the dip at lower energies corresponds to scatterings with ν_3 , which is the heavier mass eigenstate, while the dip at higher energies corresponds to the lighter ν_1 and ν_2 . This also explains why the higher energy dip is deeper, as more neutrino states can satisfy the corresponding resonance condition. Additionally, since the resonance condition can be met at different redshifts, the

⁹We are using natural units throughout this paper, so h_0^{-1} is in fact c/h_0 , i.e. $h_0^{-1} \sim 4.3 \text{ Gpc} (\sim 10^{23} \text{ km})$.

dip is broadened to smaller energies. Lastly, notice the bump at energies below the dips, which is due to energy conservation: for every interaction, a cosmogenic neutrino gets downscattered while a $C\nu B$ neutrino gets upscattered. All in all, the typical spectral features arising from νSI are a depletion of the flux for some energies followed by an enhancement at lower energies. As pointed out in Ref. [61], this double-dip plus bump spectral feature is difficult to explain away with modified astrophysics or random fluctuations since the position of the dips and the bump are mostly fixed by external data i.e. neutrino oscillations and cosmology.

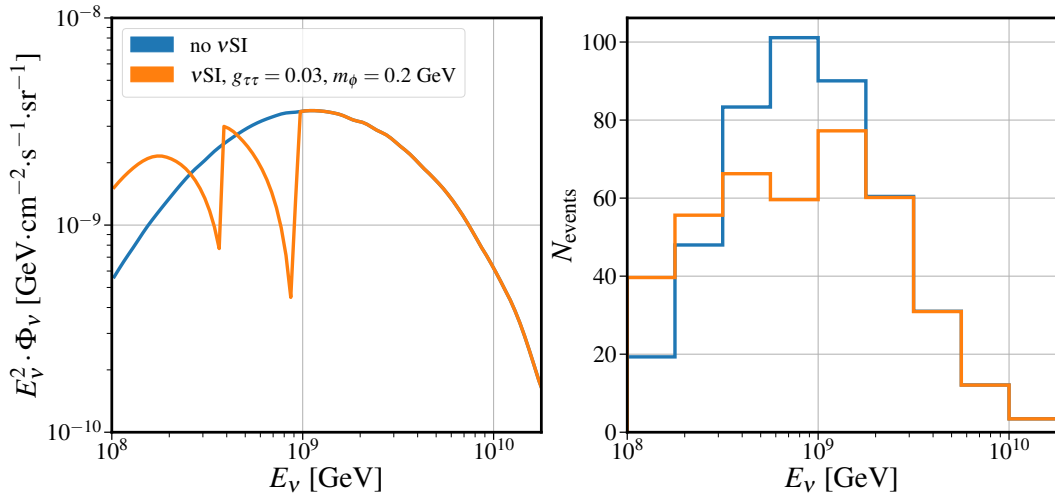


Figure 3: On the left panel we present the single-flavor cosmogenic neutrino flux at the Earth for $\gamma = 2.5$, $m = 3$ and $E_{\max} = 250$ EeV without νSI (blue) and with νSI for $g_{\tau\tau} = 0.03$ and $m_\phi = 0.2$ GeV (orange). On the right panel we have the corresponding event distributions at GRAND (10-year exposure).

4.2 Pseudo-Dirac neutrinos (PD ν)

Another BSM scenario that could potentially leave an observable imprint in the cosmogenic neutrino spectrum is if neutrinos have a pseudo-Dirac nature [64–66]. Pseudo-Dirac fermions are fundamentally Majorana fermions which behave basically like Dirac particles for terrestrial experiments because of the extremely small mass-squared difference δm^2 between their active and sterile components. Theoretically, this scenario amounts to neutrinos receiving most of their mass from a Dirac mass term m_D , but also having a small Majorana mass μ , the mass Lagrangian being

$$-\mathcal{L} \supset m_D \bar{\nu}_L \nu_R + \mu \bar{\nu}_R^c \nu_R, \quad (8)$$

where ν_L are left-handed neutrinos, part of the SM lepton doublets, and ν_R are right-handed SM singlets. The small μ lifts the degeneracy of the mass eigenvalues, so in the end we have pairs of eigenstates with almost degenerate masses. Since this also entails a soft breaking of the accidental SM lepton number symmetry, one could argue that pseudo-Dirac neutrinos could be connected to quantum gravitational effects, which are expected to break global symmetries [67]. Furthermore, there are many well-motivated models in the literature that can predict pseudo-Dirac neutrinos [68–75].

In this scenario, active-sterile oscillations are expected to modify the standard oscillations [76] leading to observable effects in experiments [77–80]. The effect is proportional to

the tiny mass squared splitting δm^2 so one needs astrophysical to cosmological distances for these oscillations to develop. This makes cosmogenic neutrinos interesting to search for these oscillations.

The evolution of cosmogenic neutrinos in vacuum is governed by the Hamiltonian:

$$H_{\text{vac}}(z) = \frac{1}{E_\nu(z, E_\nu)} V^\dagger M_{\text{diag}}^2 V,$$

where $E_\nu(z, E_\nu) = E_\nu(1+z)$ is the neutrino energy at redshift z when E_ν is the neutrino energy at the Earth and M_{diag}^2 is a 6×6 diagonal mass matrix with entries

$$m_{i\pm}^2 = m_i^2 \pm \frac{\delta m_i^2}{2}, \quad i = 1, 2, 3, \quad (9)$$

which correspond to the mass eigenstates which are a maximal mixture of active and sterile components

$$\nu_i^+ = \frac{1}{\sqrt{2}}(\nu_{ia} + \nu_{is}), \quad (10)$$

$$\nu_i^- = \frac{-i}{\sqrt{2}}(\nu_{ia} - \nu_{is}), \quad (11)$$

so the 6×6 unitary matrix V can be parametrized as [76]

$$V = \frac{1}{\sqrt{2}} \begin{pmatrix} U & 0 \\ 0 & U_N \end{pmatrix} \begin{pmatrix} \mathbf{I}_3 & i\mathbf{I}_3 \\ \phi & -i\phi \end{pmatrix}, \quad (12)$$

where U and U_N are, respectively, the PMNS and another unitary mixing matrix that diagonalize the active and sterile sectors, $\phi = \text{diag}(e^{-i\phi_1}, e^{-i\phi_2}, e^{-i\phi_3})$ is a diagonal phase matrix and \mathbf{I}_3 is the 3×3 identity matrix. The flavor states can be written in terms of the almost degenerate mass eigenstates as

$$\nu_\alpha = \frac{U_{\alpha i}}{\sqrt{2}}(\nu_i^+ + i\nu_i^-), \quad \alpha = e, \mu, \tau \quad (13)$$

so the flavor oscillation probabilities will, in general, depend on the two larger mass splittings $\Delta m_{21}^2 \equiv m_2^2 - m_1^2 \simeq m_{2\pm}^2 - m_{1\pm}^2 \sim 7.5 \times 10^{-5} \text{ eV}^2$ and $|\Delta m_{31}^2| \equiv |m_3^2 - m_1^2| \simeq |m_{3\pm}^2 - m_{1\pm}^2| \sim 2.5 \times 10^{-3} \text{ eV}^2$ [81] as well as on the active-sterile splitting δm_i^2 . Since $\delta m_i^2 \ll \Delta m_{21}^2, |\Delta m_{31}^2|$ we will assume, for simplicity, they are all degenerate and equal to δm^2 . Furthermore, the oscillation length is defined as

$$L_{\text{osc}} = \frac{4\pi E_\nu}{\Delta m^2} \approx 8 \times 10^{-9} \left(\frac{E_\nu}{1 \text{ EeV}} \right) \left(\frac{10^{-5} \text{ eV}^2}{\Delta m^2} \right) \text{ Gpc}, \quad (14)$$

where $\Delta m^2 = \Delta m_{21}^2, |\Delta m_{31}^2|$ or δm^2 . This is much smaller than a few Gpc (the typical scale distance traveled by a cosmogenic neutrino to Earth) for the two larger mass squared differences, so these oscillations are averaged out over cosmological distances. This also tells us that cosmogenic neutrino data can probe $\delta m^2 \sim 10^{-14} \text{ eV}^2$. Also, because the effective distance due to redshift traveled by cosmogenic neutrinos from their production point (at z_p) to Earth (at $z = 0$) can be computed as

$$L_{\text{eff}}(z_p) = \int_0^{z_p} \frac{dz}{H(z)(1+z)^2}, \quad (15)$$

the final ν_α to ν_β oscillation probability will be simply

$$P(\nu_\alpha \rightarrow \nu_\beta; z_p) = \frac{1}{2} \sum_{i=1,3} |U_{\alpha i}|^2 |U_{\beta i}|^2 \left[1 + \cos \left(\frac{\delta m^2 L_{\text{eff}}(z_p)}{2E_\nu} \right) \right], \quad (16)$$

and similarly for the antineutrino modes. This will impact the cosmogenic $\nu_\tau + \bar{\nu}_\tau$ flux that can be measured by GRAND. For the PMNS entries $U_{\alpha i}$, we fix the mixing angles and phase to the latest bestfit values from the global neutrino oscillation analysis [81].

It should be noted that, as pointed out in Ref. [80], pseudo-Dirac neutrinos traveling through the Universe feel a matter effect with the $C\nu B$ due to coherent Z -exchange, as the right-handed component is sterile under weak interactions. In the interaction basis, this matter Hamiltonian reads:

$$H_{\text{mat}}(z) = \frac{G_F}{\sqrt{2}} n_{C\nu B}(z) \begin{pmatrix} \mathbf{I}_3 & 0 \\ 0 & 0 \end{pmatrix}, \quad (17)$$

where $n_{C\nu B}(z) = n_{C\nu B}^{(0)}(1+z)^3$ $C\nu B$ number density at redshift z , which reduces as the universe expands. As stated in Ref. [80], this matter effect tends to drive the active-sterile mixing out of the maximal regime, thus damping the oscillatory pattern that could be resolved in neutrino telescopes. However, the size of this effect is negligible when compared with the vacuum term if no sizable $C\nu B$ overdensities are considered. Indeed, the relative size of the matter and vacuum Hamiltonian is given by:

$$\frac{\|H_{\text{mat}}\|}{\|H_{\text{vac}}\|} \sim 1.4 \times 10^{-3} \left(\frac{10^{-14} \text{ eV}^2}{\delta m^2} \right) \left(\frac{E_\nu}{1 \text{ EeV}} \right) (1+z)^4. \quad (18)$$

Notice how the different redshift dependence of the vacuum and matter Hamiltonian makes the matter effect stronger at higher redshifts. In order to make sure that neglecting the matter effect is a good approximation in all of the parameter space relevant for GRAND, we have performed the full computation of the oscillation probability, that is, we have explicitly solved the time-dependent Schrödinger equation $\frac{d}{dt} |\nu_a(t)\rangle = -i[H_{\text{vac}}(t) + H_{\text{mat}}(t)]_{ab} |\nu_b(t)\rangle$, finding that H_{mat} can be safely neglected in the δm^2 interval relevant for our analysis.

Let us now discuss the robustness of the bounds that can be derived on the $\text{PD}\nu$ mass-splittings δm^2 from the diffuse analysis. Indeed, the optimal method of deriving robust bounds on δm^2 would be to identify specific point sources at known redshifts, so that the effective baseline (15) is fixed and the only free parameter in the survival probability is δm^2 . However, when analyzing the diffuse flux, assumptions on the source distribution must be taken, which might render the derived constraints on δm^2 dependent on said assumptions. However, here we argue that this model-dependence is not as pronounced as it would naively seem. The main reason why this is the case can be seen from the left panel of Fig. 4, where we plot the effective neutrino baseline L_{eff} as a function of the redshift z_p . Indeed, L_{eff} quickly saturates to ~ 2 Gpc such that all neutrinos coming from $z_p \gtrsim 0.5$ effectively travel the same distance from the point of view of the oscillation probability. Alternatively, in the right panel, we show the (normalized) L_{eff} distribution of simulated events for three different source evolutions (see Eq. (2)): $m = 3$ (solid blue), $m = 0$ (dashed orange) and $m = -3$ (dotted green). In all of the three cases, the distributions are clearly peaked at $L_{\text{eff}} \simeq 2$ Gpc, with the sharpness of the peak decreasing with m , which can be intuitively understood as a smaller m increasingly suppresses sources at redshifts for which $L_{\text{eff}} \sim \text{Gpc}$. However, even for the weakest source evolution considered in Fig. 4, i.e. $m = -3$, the fraction of neutrinos whose $L_{\text{eff}} \in [1, 2.25]$

Gpc is 65%, which increases to 86% and 97% for $m = 0$ and $m = 3$, respectively. Therefore, for a wide range of source evolutions, a large proportion of neutrinos have very similar \sim Gpc oscillation baselines, making the analysis of $\text{PD}\nu$ quite robust even in the context of a diffuse flux measurement.

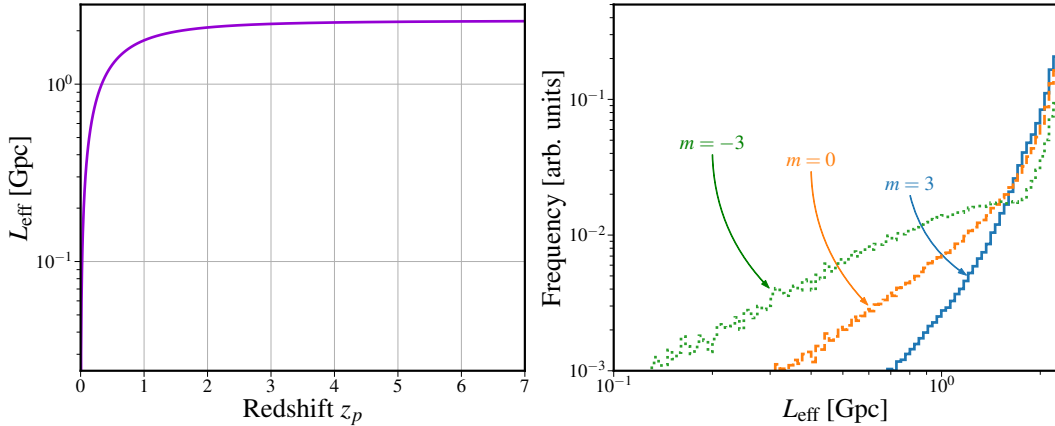


Figure 4: On the left panel we show how L_{eff} changes as a function of the redshift z_p of the production point. On the right panel we can see for different values of the source evolution parameter $m = -3$ (dotted green), $m = 0$ (dashed orange) and $m = 3$ (solid blue) the distribution of events as a function of L_{eff} , where we fixed $\gamma =$ and $E_{\text{max}} = 250$ EeV.

We compute the cosmogenic flux in the presence of $\text{PD}\nu$ by simulating the production of cosmogenic neutrinos as outlined in Sec. 2 and reweighting each event by its corresponding survival probability, given by Eq. (16). In Fig. 5 we compare the cosmogenic flux and expected number of events at GRAND considering SM physics (blue) and $\text{PD}\nu$ (orange). It is clear that active-sterile oscillations produce an oscillatory pattern of dips in the spectrum when the condition $\delta m^2 L_{\text{eff}} / (2E_\nu) \simeq (2n + 1)\pi$ is met, since the active-sterile conversion is maximal. The first oscillation dip (the one appearing at higher energies) is of special relevance in order to disentangle the effect of $\text{PD}\nu$ from astrophysics or statistical fluctuations. Indeed, it is the widest dip and thus the easiest to resolve, given the energy resolution. As it can be seen from Fig. 5, only the first oscillation dip is appreciable in the distribution of the number of events, while subsequent oscillations are not resolved and instead amount to an overall decrease on the number of events at the lowest energy bins. In contrast to the νSI scenario, the spectral dip generated by $\text{PD}\nu$ is not accompanied by a bump and its position is not given by any external input, which makes the sensitivity very dependent on observing a suppressed number of events in some energy bins. This kind of signal, while not necessarily easy to mimic by varying the astrophysics, does become susceptible to random underfluctuations if the flux measurement is statistically limited.

4.3 Neutrinos Scattering on Ultra-light Scalar Dark Matter (νDM)

There is abundant evidence for the existence of Dark Matter (DM) coming from observations related to gravity that span a wide range of scale distances, from galaxy sizes to the observable Universe. Yet we have no clue about the particle nature of DM and how the dark sector communicates with the SM one. An interesting possibility is that DM could be made of ultra-light scalars, a conceivable fuzzy DM candidate. Being macroscopically delocalized, fuzzy

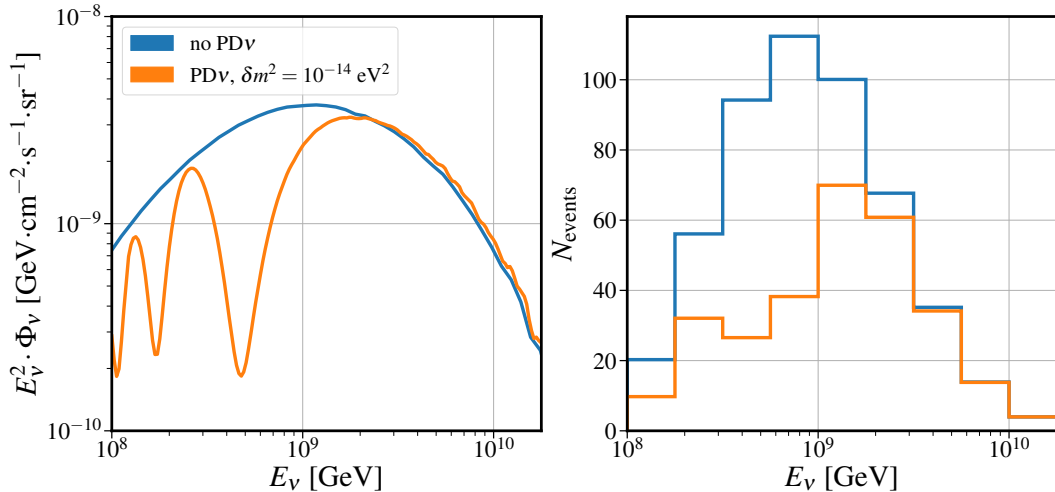


Figure 5: On the left panel we present the single-flavor cosmogenic neutrino flux at the Earth for $\gamma = 3, m = 3$ and $E_{\text{max}} = 250$ EeV without $\text{PD}\nu$ (blue) and with $\text{PD}\nu$ for $\delta m^2 = 10^{-14}$ eV² (orange). On the right panel we have the corresponding event distributions at GRAND (10-year exposure).

DM can potentially alleviate some problems of ΛCDM related to small-scale: the cusp vs. core, the missing satellites, and the too-big-to-fail problems [82]. The production of such a light DM could be achieved in the early Universe, for instance, by means of the misalignment mechanism [83–85].

If neutrinos provide a portal to these ultra-light scalar fields, a general effect is that their masses and mixings receive corrections that are time-dependent, potentially affecting neutrino oscillations [82, 86–95]. Furthermore, it has also been proposed that neutrino interactions with ultra-light dark matter could be responsible for the phenomenon of neutrino oscillations even in the presence of massless neutrinos [95]. In this kind of scenario, neutrinos would acquire a “refractive” mass from the matter effect with the DM, leading to very rich phenomenology, as neutrino masses would not only showcase an energy dependence but also depend on the dark matter density. One of the best probes for such interactions is the measurement of astrophysical neutrinos propagating through cosmological distances, as they traverse large column depths of DM on their way to Earth. Since this kind of interaction could render the Universe opaque to these neutrinos, the observations of Supernova neutrinos [96–99], as well as high-energy neutrinos at IceCube [100] can be employed to place constraints on the parameter space [61]. Alternatively, interactions of cosmic neutrinos with DM during the evolution of the Universe can leave an imprint on the CMB and matter power spectrum, which can be harnessed to constrain νDM interactions [101–104].

We will consider here a model where neutrinos interact with ultra-light scalar bosons S and their antiparticles \bar{S} , which could act as cold (non-relativistic) DM, via a new fermion χ that could be either a Dirac or a Majorana particle [95]. A single scalar is enough for our purposes here as we do not require the ultra-light scalars to explain neutrino masses and mixings. The

Lagrangian describing neutrino scattering on DM in the mass basis can take the form ¹⁰

$$\mathcal{L} \supset -y_k \bar{\chi}_R \nu_{kL} S + y_k^* \bar{\nu}_{kL} \chi_R S^* , \quad (19)$$

with $k = 1, 2, 3$. The DM particles have mass $m_S \ll \text{eV}$ and the fermions χ have mass $m_\chi \gg m_S$. The scalars' contribution to the energy density of the Universe is

$$\rho_S = m_S(n_S + n_{\bar{S}}) , \quad (20)$$

where n_S ($n_{\bar{S}}$) is the scalar S (\bar{S}) number density, and we will suppose ρ_S to be equal to the entire cosmological DM energy density $\Omega_{\text{DM}} = 0.25$ when solving the extragalactic transport equation (see Appendix A). It should be noted that we will only consider the interactions of cosmogenic neutrinos with the cosmological dark matter abundance. Even though galactic scales are much smaller than cosmological scales, the high DM overdensity inside the Milky Way's halo compensates for this hierarchy, thus rendering the galactic and cosmological DM column depths comparable. For the sake of simplicity, we have opted not to simulate ν DM interactions within the galactic halo; therefore, our treatment is on the conservative side. However, this kind of interactions in the galactic halo would generate interesting signatures, such as a non-isotropic flux at Earth due to the Solar System being off-center of the DM halo.

For a detailed description of neutrino creation and annihilation processes within this model, we present in Appendix B the differential cross section for these scatterings. Since for the parameter values relevant for our setup, the cross section is resonant only in a very narrow energy window unresolvable by GRAND, we will separately consider two regimes of interest: the parameter space region in which the center-of-mass energy is well above the resonance condition $s = 2E_\nu m_S \gg m_\chi^2$ (i.e. light mediator) and the region in which $s = 2E_\nu m_S \ll m_\chi^2$ (i.e. heavy mediator). In these two regimes, the interaction rate $\Gamma_{\nu S}$ reads

$$\Gamma_{\nu S} = n_S \sigma_{\nu S} + n_{\bar{S}} \sigma_{\nu \bar{S}} = \frac{1}{2} \rho_S \begin{cases} \frac{y^4}{4\pi m_\chi^4} E_\nu & E_\nu \ll \frac{m_\chi^2}{2m_S} , \\ \frac{y^4 \left(2 \log \left(\frac{2E_\nu m_S}{m_\chi^2} \right) - 1 \right)}{64\pi m_S^2 E_\nu} & E_\nu \gg \frac{m_\chi^2}{2m_S} , \end{cases} \quad (21)$$

where, for simplicity, we have dropped the mass indices in the coupling and assumed equal number densities for S and \bar{S} . Notice how, in the heavy mediator regime, the interaction rate is independent of the scalar DM mass m_S , while in the light mediator regime, $\Gamma_{\nu S}$ has a very mild logarithmic dependence on the fermion mediator mass m_χ .

Unlike the ν SI scenario, in which the spectral dip originating from the resonance was crucial for the sensitivity, this scenario does not rely on this feature due to two reasons: first of all, the resonance is too narrow to be resolved and secondly, due to the DM being ultralight, the very large number densities greatly enhance the interaction rate such that, even for small couplings and non-resonant energies, the flux can still be greatly modified. In Fig. 6 we show the effect of ν DM interactions in the cosmogenic neutrino flux for the two regimes of Eq. (21). Due to the different energy dependence of the interaction rate, the suppression is more pronounced towards lower or higher energies, depending on the regime. It is evident that the effect of ν DM interactions does not generally lead to pronounced spectral features, such that the shape of the

¹⁰This kind of effective Lagrangian can be accomplished in a gauge invariant way by UV-complete models which may involve, for e.g., pairs of vector-like fermions which are SM singlets or SM triplet fermions (see Ref. [59] and references therein).

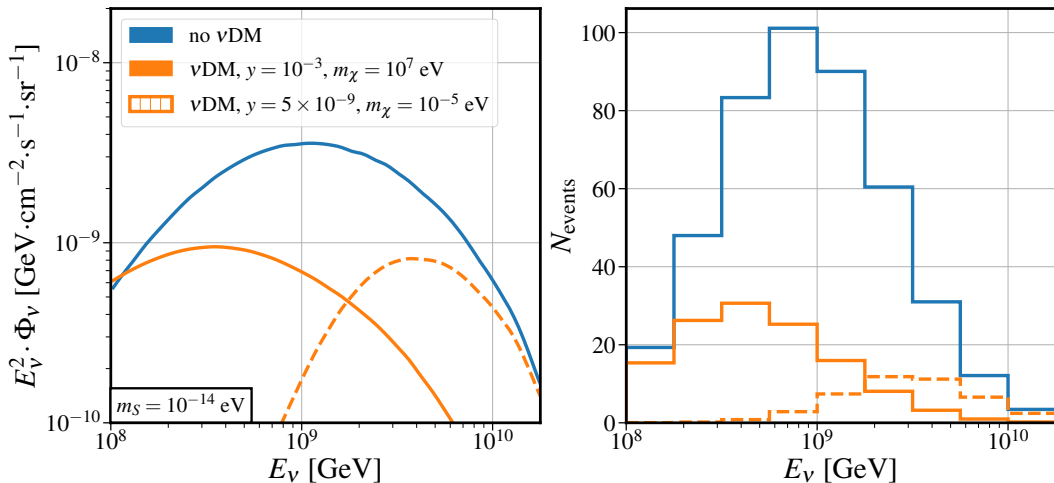


Figure 6: On the left panel we present the single-flavor cosmogenic neutrino flux at the Earth for $\gamma = 3$, $m = 3$ and $E_{\max} = 250$ EeV without ν DM interaction (blue) and with ν DM interaction for $y = 10^{-3}$ and $m_\chi = 10^7$ eV (solid orange) and for $y = 5 \times 10^{-9}$ and $m_\chi = 10^{-5}$ eV (dashed orange), both for $m_S = 10^{-14}$ eV. On the right panel we have the corresponding event distributions at GRAND (10-year exposure).

modified flux might be somewhat degenerate with astrophysical parameters. However, even for relatively small couplings, the flux suppression induced by ν DM interactions cannot be offset by even the most optimistic astrophysical assumptions (e.g. a very strong source evolution). Therefore, the sensitivity to this scenario does not rely on resolving specific spectral features and simply hinges on a positive detection of the cosmogenic flux, which would allow us to rule out parts of the parameter space in which ν DM interactions opaque the Universe to cosmogenic neutrinos. This in turn means that GRAND’s exclusion power will not be sizably reduced even if the flux measurement is statistically limited, as only a handful of events can already place robust constraints.

We compute the cosmogenic neutrino flux at Earth in the presence of ν DM by solving the transport equation using a modified version of the `nuSIprop` [61] code employed in the ν SI analysis, where we have replaced the collision terms of the ν SI setup by our own computations in the ν DM scenario, as well as replaced the C ν B number density by the cosmological DM number density. For some choice of astrophysical parameters, the cosmogenic flux at Earth can then be calculated by specifying the coupling y_τ , the DM mass m_S , and the mediator mass m_χ .

5 Analysis and Results

In order to evaluate GRAND’s sensitivity to the BSM models we discussed in section 4, we generate mock data under the hypothesis of SM physics. We will do this by computing the cosmogenic neutrino spectrum for two benchmark values of the astrophysical parameters (γ , E_{\max} and m): a more optimistic choice, which corresponds to $\gamma_A = 2.5$, $E_{\max,A} = 250$ EeV and $m_A = 3$ and a less optimistic choice, which corresponds to $\gamma_B = 2.5$, $E_{\max,B} = 250$ EeV and $m_B = 0$. Notice that, since the source composition and evolution are degenerate (see last

panel of Fig. 1), these benchmark scenarios can be viewed as representative of cases in which the sources have heavier compositions and a stronger source evolution. We note, however, that many astrophysical models [6, 9, 105–107] predict a flux well below the sensitivity of GRAND. Nevertheless, the neutrino flux at EeV energies is highly uncertain; it may vary about 2 orders of magnitude depending on the evolution of the EECR sources and mass composition [6, 36]. There may be additional components of $E_\nu \gtrsim 1$ EeV neutrinos produced by largely unconstrained sources [10, 108, 109]. In Fig. 7 we show the flux predictions for our two benchmark points as a function of the neutrino energy in the range $(10^8 - 3 \times 10^{10})$ GeV. Notice how our more optimistic benchmark scenario is already in slight tension with the constraints from the recent IceCube cosmogenic search [110]. However, the data point KM3-230213A may be an indication that the true cosmogenic flux may be more consistent with our more optimistic scenario, although this interpretation is in tension with IceCube’s non-observation of similar events [111].

We then compute the prediction for the number of $(\nu_\tau + \bar{\nu}_\tau)$ events in each of the 9 energy bins we consider: $\hat{N}_k = \hat{N}_k(\gamma_{A,B}, E_{\max,A,B}, m_{A,B})$ is the standard mock data prediction for one of the benchmark values for the cosmogenic spectrum and $N_k(\theta, \gamma, E_{\max}, m)$ is the corresponding prediction for a given BSM scenario which will also depend on θ , the parameters of the model, as well as the flux parameters γ , E_{\max} and m .

The sensitivity power of GRAND for each BSM model is then quantified by means of a test statistic, where we compare the number of events $N_k \equiv N_k(\theta, \gamma, m)$ predicted for a BSM model at a given value of the model parameters θ , with the mock data value \hat{N}_k . Our test statistic is defined by the Poisson log-likelihood

$$\begin{aligned} \lambda(\theta, \gamma, E_{\max}, m) &= -2 \log \mathcal{L}(\theta, \gamma, E_{\max}, m) \\ &= 2 \sum_{k=1}^9 \left[N_k(\theta, \gamma, E_{\max}, m) - \hat{N}_k + \hat{N}_k \log \frac{\hat{N}_k}{N_k(\theta, \gamma, E_{\max}, m)} \right], \end{aligned} \quad (22)$$

so GRAND’s sensitivity for fixed values of the BSM parameters θ will be given by the value of λ after minimizing over the three astrophysical parameters. We will vary them in the range $m \in [-3.0, 3.0]$, $\gamma \in [2.0, 3.0]$ and $E_{\max} \in [10^2, 10^5]$ EeV. This procedure allows us to construct the experiment’s sensitivity region at a certain confidence level for the parameters of each BSM model.

An important observation is the fact that, while changing the source evolution parameter m amounts to a reweighting of the simulated events, changing γ and E_{\max} requires launching a new simulation, as the cosmogenic flux depends on these quantities in a non-parametric fashion. Therefore, in order to vary these two astrophysical parameters within their aforementioned ranges, we first generate several spectrum templates for different choices of γ and E_{\max} and then we proceed to scan the parameter space θ of the BSM setup along with the source evolution m . For each point in the scan, we compute the test statistic as in Eq. (22) for all of the spectrum templates, keeping the smallest value, i.e., we profile the test statistic over γ and E_{\max} . After a subsequent profiling over m , we compute the sensitivity of the profiled test statistic $\lambda(\theta)$ under the assumption that it is distributed as a χ^2 with degrees of freedom equal to the dimension of θ .

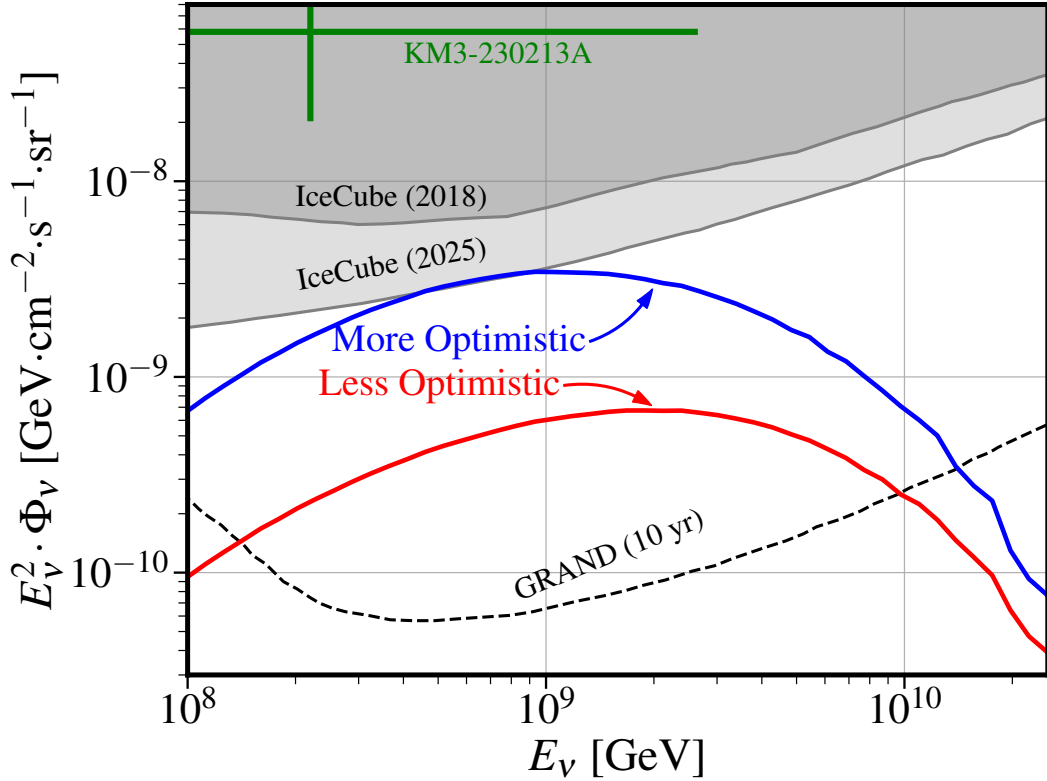


Figure 7: Single-flavor cosmogenic flux at GRAND for the two benchmark values of the astrophysical parameters, $\gamma_{A,B} = 2.5$, $E_{\max,A,B} = 250$ EeV and $m_A=3$ (more optimistic choice, in blue) and $m_B = 0$ (less optimistic choice, in red). We also show the two IceCube upper limits at 90% C.L. (dark and light gray-shaded regions) [110, 112] and GRAND’s projected 10-year sensitivity curve (dashed line) [21]. We also show as a reference the data point KM3-230213A [7] with 1σ uncertainties in its normalisation.

ν SI results

Let’s start the discussion of our results with the ν SI model. There are already several limits on these lepton number violating scalar neutrino couplings. Let’s start from laboratory bounds coming from meson M decays, i.e. from $M \rightarrow \ell_\alpha \nu_\beta \phi$ with $m_\phi < m_M - m_{\ell_\alpha}$. In the lower mass range, kaons decays are the main reason for the limits $(\sum_\alpha |g_\phi^{e\alpha}|^2)^{1/2} \lesssim 7 \times 10^{-3}$, for $m_\phi \lesssim 200$ MeV, and $(\sum_\alpha |g_\phi^{\mu\alpha}|^2)^{1/2} \lesssim 2.2 \times 10^{-2}$, for $m_\phi \lesssim 100$ MeV [113]. In the range $0.1 < m_\phi/\text{GeV} < 2$ limits on $|g_\phi^{\alpha\beta}|$ from $M = K, D_s$ and B leptonic decays as well as from invisible $Z \rightarrow \nu_\alpha \nu_\beta \phi$ decays are much weaker [114]. There are also limits from $\tau \rightarrow \ell_\alpha \nu_\alpha \nu_\tau \phi$ on $(\sum_\alpha |g_\phi^{\tau\alpha}|^2)^{1/2} < \mathcal{O}(1)$, for $m_\phi \lesssim 0.75$ MeV [114, 115]. Neutrino self-interaction can also cause neutrinoless double beta decay as $(A, Z) \rightarrow (A, Z+2) + 2e^- + \phi$, provided that ϕ is lighter than the Q -value of the decaying nucleus. Thus KamLAND-Zen [116] and EXO [117] can set the limits $|g_\phi^{ee}| \lesssim 10^{-3}$ (10^{-5}) for $m_\phi \lesssim 2$ (0.2) MeV [118]. Coherent neutrino scattering can impose bounds on couplings of the order 10^{-4} , if ϕ couples to quarks and couplings to neutrinos are taken to be flavor universal [119, 120]. Luminosity and deleptonization constraints imposed on the observation of SN1987A exclude the range $2.1 \times 10^{-9} \lesssim |g_\phi^{ee}| \times (m_\phi/\text{MeV}) \lesssim 1.6 \times 10^{-6}$,

$5.5 \times 10^{-9} \lesssim |g_{\phi}^{\mu\mu,\tau\tau}| \times (m_{\phi}/\text{MeV}) \lesssim 1.1 \times 10^{-6}$ and $2.3 \times 10^{-8} \lesssim |g_{\phi}^{e\mu,e\tau}| \times (m_{\phi}/\text{MeV}) \lesssim 6.6 \times 10^{-7}$, for $m_{\phi} \in [10, 500] \text{ MeV}$ [121]. Bounds from Big Bang Nucleosynthesis also exist, but they only apply for $m_{\phi} \lesssim 1 \text{ MeV}$ [59, 122]. Lastly, it has been shown that sufficiently strong νSI may affect the CMB power spectrum and partially alleviate the Hubble tension [123]. In Fig. 8, along with the different constraints, we show the region of parameter space, dubbed $\text{MI}\nu$ (Moderately Interacting Neutrinos), where this solution can be achieved. However, it should be noted that, while CMB and BAO data do showcase a preference for νSI , it has been recently shown that this preference goes away once the information from the full-shape analysis of the matter power spectrum is added [124].

Our results for νSI are shown in Fig. 8. In this case $\theta \equiv \{g_{\tau\tau}, m_{\phi}\}$, which we vary in the range $g_{\tau\tau} \in [10^{-3}, 1]$ and $m_{\phi} \in [10^7, 10^9] \text{ eV}$. In this figure, we show the sensitivity we derived for GRAND (colored dashed lines) with the current constraints (colored solid lines) from other experiments. We have also included the prospective sensitivity of the Cherenkov part of IceCube-Gen2 [61] as a reference. We can see that IceCube-Gen2 has better sensitivity for the coupling $g_{\tau\tau}$ than GRAND's; however, for a lighter mediator, i.e., $m_{\phi} \sim$ a few MeV to a few tens of MeV. This is because IceCube-Gen2, using the Cherenkov effect, is expected to detect lower energy neutrinos. Moreover, as the resonant cross section $\sigma_{\text{res}} \sim 1/m_{\phi}^2$ is larger for lighter mediators, the imprints of νSI in the IceCube-Gen2 spectrum are easier to detect, i.e., they lead to more pronounced spectral features. This aspect, combined with the superior energy resolution of Gen2 compared to GRAND, leads to the former being able to set stronger bounds on $g_{\tau\tau}$ by more than one order of magnitude, even when Gen2's statistics can potentially be comparable to GRAND's. We also plot as a gray dotted line the parameter space in which the mean free path, estimated as $\lambda_{\text{MFP}}^{-1} \sim \frac{g_{\tau\tau}^2}{m_{\phi}^2} n_{\nu}$ is equal to the typical $\sim h_0^{-1}$ ($\sim \text{Gpc}$) baselines traversed by cosmogenic neutrinos. This serves as a rough sensitivity limit for high-energy neutrino observatories, as couplings below the gray dotted line would barely produce any modification on high-energy extragalactic neutrinos. As pointed out in Ref. [61], IceCube-Gen2 will have enough constraining power to probe this sensitivity limit. Remarkably, also GRAND (under optimistic flux assumptions) will also be able to probe along this maximum sensitivity line.

However, Fig. 8 also shows GRAND's complementarity to other experiments, as it can potentially constrain a previously unexplored region of the parameter space. The shape of GRAND's sensitivity can be easily understood. When the mediator is too light, the spectral dip induced by the resonant enhancement of the cross section falls at neutrino energies below GRAND's sensitivity threshold, which is the reason why the constraint sharply drops for $m_{\phi} \lesssim 100 \text{ MeV}$. On the contrary, even when the mass of the mediator is too large such that the dip from the resonant cross section falls above GRAND's energy sensitivity, cosmogenic neutrinos get down-scattered to lower energies, thus producing a bump in the spectrum to which GRAND can still be somewhat sensitive. For this reason, the sensitivity curve falls in a slightly smoother way as one moves to larger mediator masses.

PD ν results

Next let us examine the PD ν model. In this case, there are also several limits on the mass splitting δm^2 from different experimental data. Solar neutrinos constrain the mass splitting to be in the region $\delta m^2 \lesssim 10^{-12} \text{ eV}^2$ [125, 126] while atmospheric neutrinos provide the much weaker bound $\delta m^2 \lesssim 10^{-4} \text{ eV}^2$ [127]. An analysis of neutrinos from SN1987A can exclude

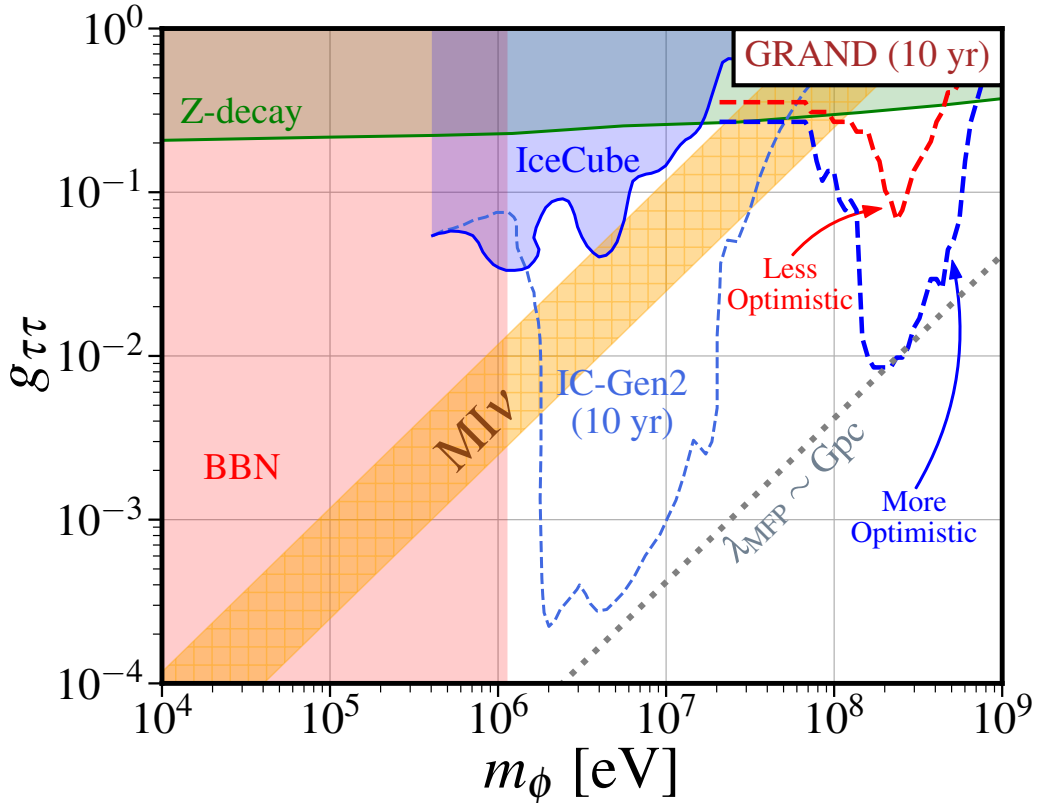


Figure 8: Future sensitivity of GRAND (10-year exposure) on the ν SI parameter space $g_{\tau\tau}$ versus m_ϕ . The dashed blue (red) curve shows the sensitivity of GRAND for the more (less) optimistic benchmark values of the astrophysical parameters. We also show the Z decay (green) and BBN (red) 95% CL bounds as well as the constraints from IceCube HESE 7.5-year data (blue) and the IceCube-Gen2 10-year sensitivity curve, which are taken from Ref. [61]. For reference, we present in yellow the region where the tension in the Hubble parameter can be alleviated by ν SI [123], labeled $MI\nu$.

smaller splittings but for the narrow range $\delta m^2 \in [2.55, 3.01] \times 10^{-20} \text{ eV}^2$ [77]. IceCube data recently allowed for limits to be set in the range $\delta m^2 \in [10^{-21}, 10^{-16}] \text{ eV}^2$ [79, 128, 129]. In Fig. 9 we show GRAND's complementary sensitivity to the range $\delta m^2 \in [10^{-15}, 10^{-13}] \text{ eV}^2$, a range not probed by previous experiments. For comparison, we plot the forecasted exclusion power of IceCube-Gen2 [79], as well as the excluded region from solar neutrinos. Indeed, thanks to its higher energies, which suppress the oscillation frequency, GRAND can probe values of δm^2 for which active-sterile oscillations would be averaged out in IceCube. The shape of the sensitivity region can be easily understood: the δm^2 interval to which GRAND is sensitive corresponds to the values for which the first oscillation dip falls within its energy range. Instead, for smaller mass splittings, oscillations do not have the time to develop, while for larger δm^2 oscillations average out and amount to a factor two suppression of the flux normalization, which cannot be disentangled from astrophysics.

Also note the strong degradation in the sensitivity from the more optimistic scenario to the less optimistic one. Indeed, in the latter case, the number of events per bin is ~ 10 or lower, which does not yield strong discriminating power against a signal that amounts to depletion

in some small energy window, as statistical fluctuations can partially mimic such a signature.

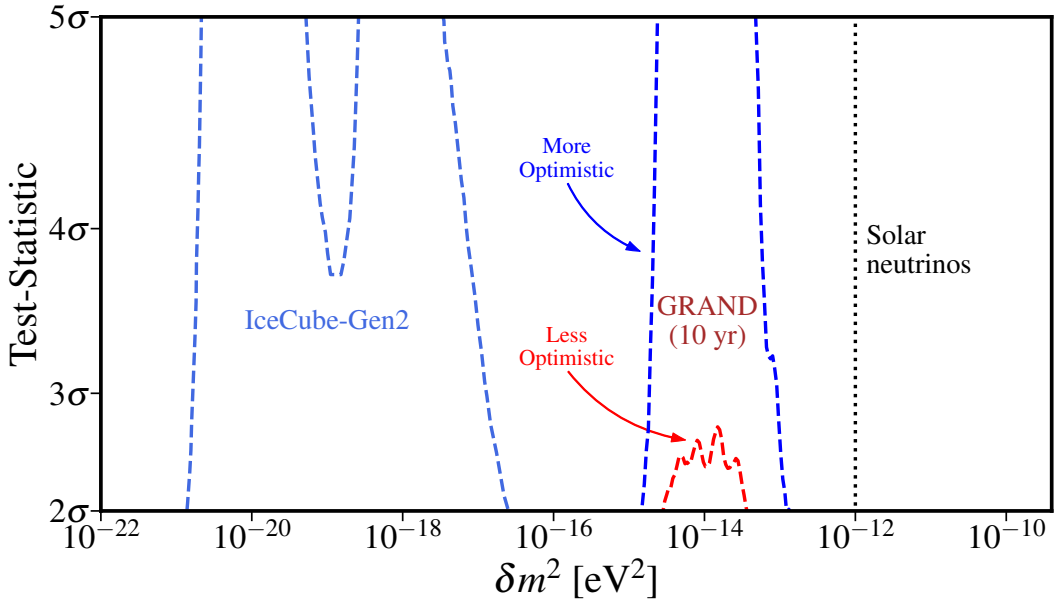


Figure 9: GRAND’s sensitivity to δm^2 for the more (less) optimistic cosmogenic flux is show in blue (red). We also show the region already excluded by solar neutrinos [125] and the region that can be probed in the future by IceCube-Gen2 [79].

ν DM results

We will now discuss the ν DM model. This kind of interaction can be constrained from measurements of neutrino fluxes that traverse galactic or even cosmological scales. In particular, bounds on the same type of interaction considered in our work were derived in Ref. [95] employing the IceCube measurement of neutrinos from the blazar TXS 0506+056 and from SN1987A. The mere observation of neutrinos coming from sources at known distances allows us to constrain the strength of ν DM interactions by requiring the Universe to not be opaque for such neutrinos. It is also possible to constrain ν DM from observations of the matter power spectrum at small scales from the Ly- α forest, the Milky Way’s satellites, or even the CMB, since diffusion damping within the neutrino-dark matter coupled fluid in the early Universe suppresses power below the damping scale [101–104].

Our results for GRAND’s sensitivity to ν DM are summarized in Fig. 10. Since we have separated this setup into two regimes (heavy and light mediators), we present our results in the two panels of Fig. 10. Notice the different horizontal axis labels, since each of the two regimes probes very different parts of parameter space (see Eq. (21)). Indeed, as outlined in Section 4, when the neutrino energy is below resonance, the interaction rate is only given by the ratio y/m_χ and is independent of the DM mass m_S (as long as the condition $E_\nu \gg \frac{m_\chi^2}{2m_S}$ is met), while in the regime above resonance, the interaction rate is mostly set by y^2/m_S , while retaining only a logarithmic dependence on the mediator mass m_χ . We also plot the constraints from IceCube and SN1987A derived in Ref. [95] for comparison. In the heavy mediator regime we also plot the bound arising from the observation of the matter power spectrum at small scales [102, 103]

via the Lyman- α forest and the Milky Way’s satellites. Due to the ultralightness of our DM candidate, the cross section grows linearly with temperature, in stark contrast with the $\propto T^0$ and $\propto T^2$ behaviors commonly adopted in the literature when analyzing ν DM in cosmological contexts. Consequently, it is not entirely straightforward to recast the bounds available in the literature into our model. As a rough estimation, we evaluate our cross section at $\langle E_\nu \rangle = \frac{7\pi^4}{180\zeta(3)}T$ with $T \sim 250$ keV, where typically bounds on $\propto T^2$ and temperature-independent cross sections equate [102]. We then employ the bound on a T -independent cross section extracted in Ref. [103]. We do not plot the corresponding cosmological ν DM bound for the regime above-resonance. The reason is twofold: the qualitatively different behavior with temperature ($\propto T^{-1}$) precludes a simple recasting of existing constraints. In addition, this kind of interaction will cross from the light to the heavy mediator regime at some point throughout cosmological evolution, which will render the bounds extracted from cosmology very sensitive to the location of this resonance crossing.

The shape of the constraints can be intuitively understood as corresponding to isocontours of the interaction rate (see Eq. 21). Moreover, notice how, in stark contrast with the previous BSM scenarios, there is little loss of sensitivity when going from the more optimistic to the less optimistic detection scenario. As previously discussed, this is a consequence of the fact that the sensitivity stems from the mere observation of a handful of neutrinos, allowing to exclude the region of parameter space in which the ν DM interaction would exponentially suppress such neutrino flux. Regarding GRAND’s exclusion power relative to the already existing constraints, the differences can be easily understood in terms of the different energy scales of the involved neutrinos. In the heavy mediator regime (Fig. 10 upper panel), the interaction rate (21) scales with E_ν and thus GRAND, with its higher energies, will be substantially more sensitive than IceCube and SN1987A, with $O(1$ PeV) and $O(10$ MeV) neutrinos, respectively. Although a dedicated cosmological analysis of this kind of ν DM scenario is required, our naive recasting also indicates that cosmogenic neutrinos can place stronger bounds than structure formation. Conversely, in the light mediator regime, the situation is reversed, as the interaction rate scales as $1/E_\nu$, thus making SN1987A the best probe in this region of parameter space, as it involves the lowest neutrino energies. Notice how TXS 0506+056 sensitivity is comparable with GRAND’s. Even though the energy scale of the neutrino from the blazar lies in the ~ 100 TeV range, substantially below the cosmogenic neutrino scale, GRAND’s sensitivity to high redshifts overcomes the suppression of the interaction rate due to higher DM densities.

6 Final Conclusions

The scattering of EECRs with photons of the CMB and of the EBL is expected to produce as a by-product neutrinos with energies of about 1 EeV, called cosmogenic neutrinos. The cosmogenic neutrino diffuse flux, however, is highly unknown due to a number of astrophysical uncertainties concerning the properties of the primary EECR sources. Recently, the observation of a near-horizontal neutrino event of about 0.1 EeV by KM3NeT [7], which may constitute the first detection of cosmogenic neutrinos, seems to indicate that the cosmogenic neutrino flux may well be within the reach of the future radio array of antennas, such as the one proposed by the GRAND project and IceCube-Gen2. This possibility represents a great opportunity to use cosmogenic neutrinos not only to learn about these extreme astrophysical sources and probe tau neutrino properties but also to investigate BSM scenarios.

By assuming that the cosmogenic neutrino flux is in fact within the reach of these future

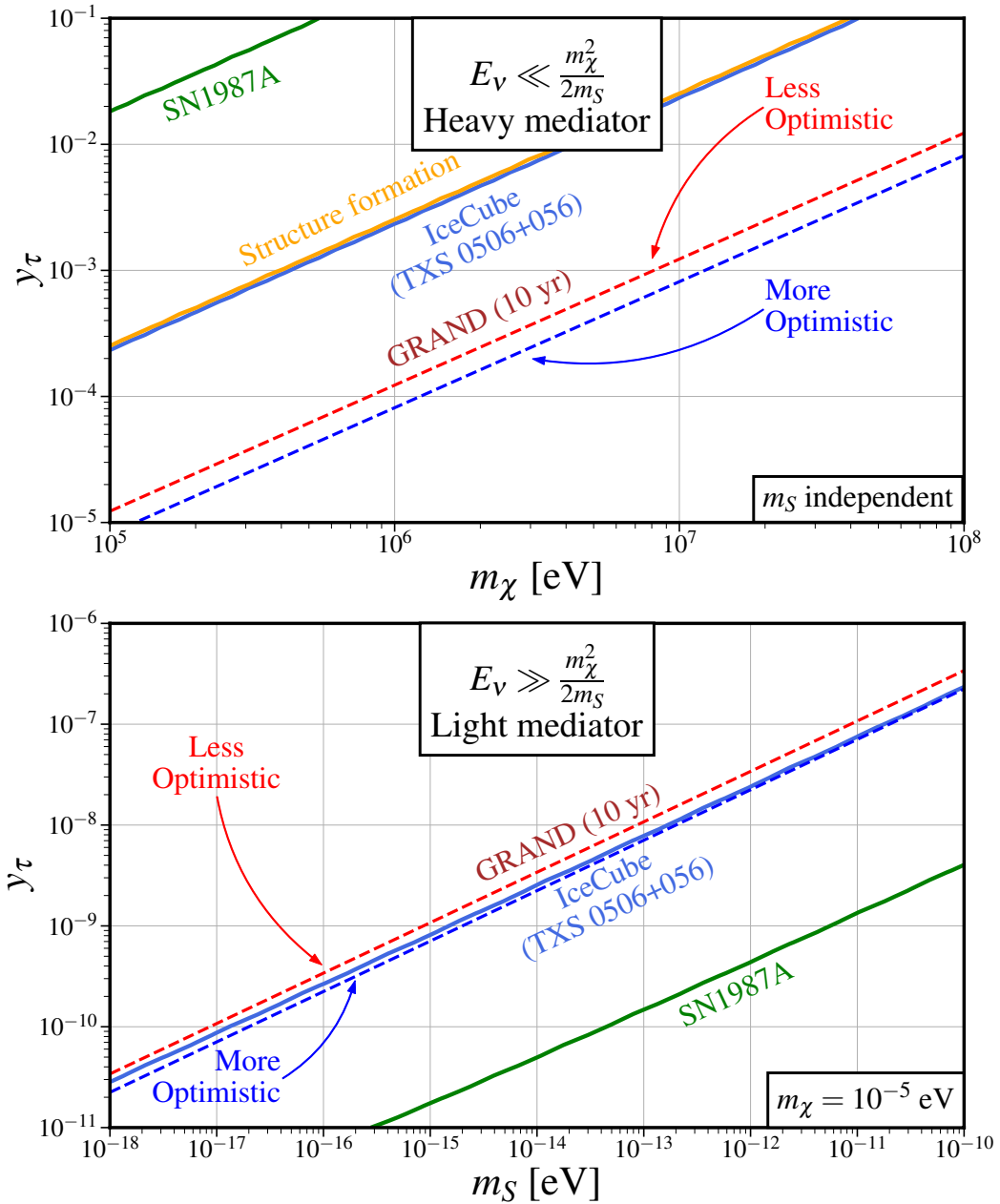


Figure 10: Here we show GRAND’s 10 year 95% CL sensitivity for the more (less) optimistic values of the astrophysical parameters in dashed blue (dashed red). In the upper (lower) panel we have the $E_\nu \ll m_\chi^2/2m_S$ ($E_\nu \gg m_\chi^2/2m_S$) regimes. We also show the limits from SN1987A (green), structure formation (yellow) and IceCube TXS 0506+056 (solid blue).

radio detectors, we investigate in our paper the sensitivity of GRAND to a few well-motivated BSM models. GRAND proposes to use radio pulse detectors to measure the cosmogenic $\nu_\tau/\bar{\nu}_\tau$ flux by means of Earth-skimming EAS produced by neutrinos that interact close to the surface producing a τ lepton as they emerge from the Earth. Since the cosmogenic neutrino flux is plagued by astrophysical uncertainties, we concentrate on models that can modify the single-

flavor ($\nu_\tau + \bar{\nu}_\tau$) diffuse cosmogenic spectrum at GRAND in a distinctive observable way, not easily mimicked by our assumptions about the astrophysical sources.

We model the cosmogenic neutrino flux by assuming a distribution of identical pure-proton sources with the same luminosity which extend up to redshift $z_{\max} = 7$ and can be described by three parameters: the power-law injection spectrum spectral index γ , the maximal proton energy E_{\max} and the source evolution parameter m . Because of known parameter degeneracies, this simple parametrization can also simulate the cosmogenic spectrum for more complex chemical compositions. We investigate two benchmark points (A and B) for the cosmogenic flux: $\gamma_A = 2.5$, $E_{\max,A} = 250$ EeV and $m_A = 3$ (more optimistic) and $\gamma_B = 2.5$, $E_{\max,B} = 250$ EeV and $m_B = 0$ (less optimistic).

We examine three BSM cases: ν SI - neutrino self-interactions (cosmogenic neutrinos interacting with the $C\nu$ B via a scalar portal), $\text{PD}\nu$ - pseudo-Dirac neutrinos (cosmogenic neutrinos are sensitive to neutrino active-sterile oscillations involving tiny mass squared splittings) and ν DM (cosmogenic neutrinos scattering on ultra-light DM).

We find that GRAND can be sensitive to a currently unconstrained parameter region of the ν SI model. It can constrain the coupling in the range $10^{-2} \lesssim g_{\tau\tau} \lesssim 10^{-1}$ for $7 \times 10^7 \lesssim m_\phi/\text{eV} \lesssim 7 \times 10^8$ in case the cosmogenic flux is consistent with benchmark A . This is complementary to what is expected to be covered by IceCube-Gen2.

According to our study, the GRAND project seems to be very sensitive to $\text{PD}\nu$ for a mass squared splitting in the range $10^{-15} \lesssim \delta m^2/\text{eV}^2 \lesssim 10^{-13}$, assuming a more optimistic cosmogenic flux. This is a currently unconstrained region for δm^2 and again a region that is complementary to the one expected to be accessible by IceCube-Gen2.

Finally, for the ν DM model, contrary to the previous scenarios, the sensitivity of GRAND is similar for both the more optimistic and the less optimistic cases. In the case of the heavy mediator scenario, due to the higher energies involved, GRAND can do substantially better than the current limits from SN1987A, IceCube and our recasting of bounds from structure formation. For a light mediator, however, GRAND limits are at most similar to IceCube and much weaker than those obtained using SN1987A data.

To conclude, we have shown that as long as the one-flavor cosmogenic neutrino flux is consistent with our two benchmark points, it can be used to constrain BSM physics at GRAND in a region of the parameter space complementary to other data.

Acknowledgments

We thank Rafael Alves Batista, Miguel Escudero, Enrique Fernandez-Martinez and Gaetano di Marco for helpful discussions. This project has received support from the European Union's Horizon 2020 research and innovation programme under the Marie Skłodowska-Curie grant agreement N° 860881-HIDDeN and N° 101086085-ASYMMETRY. L.P.S. Leal is fully financially supported by FAPESP under Contracts No. 2021/02283-6 and No. 2023/12330-7. R. Zukanovich Funchal is partially supported by FAPESP under Contract No. 2019/04837-9, and by Conselho Nacional de Desenvolvimento Científico e Tecnológico (CNPq). DNT acknowledges support from the HPC-Hydra cluster at IFT. The work of DNT was supported by the Spanish MIU through the National Program FPU (grant number FPU20/05333). DNT would like to warmly thank the Department of Mathematical Physics at USP for their hospitality, where this project was started. L.P.S. Leal would like to thank the IJCLab Theory Group for their hospitality.

A On the propagation of Cosmic Rays

For an isotropic and homogeneous distribution of cosmic ray sources, emitting particles of type i , we can define the number of particles per co-moving volume and per unit of energy E at time t as

$$n_i(t, E) \equiv \frac{dN_i(t)}{(1+z)^3 dAd\Omega dE}, \quad (23)$$

the time evolution of $n_i(t, E)$ is governed by a set of 1-dimensional transport equations [8, 130]

$$\begin{aligned} \partial_t n_i(t, E) &= \partial_E (\tilde{b}_i(t, E) n_i(t, E)) + \mathcal{L}_i(t, E) \\ &- \Gamma_i n_i(t, E) + \sum_j \int dE' \frac{d\sigma_{ji}(E, E')}{dE} n_j(t, E'), \end{aligned} \quad (24)$$

where $E = E(t, \epsilon)$, $H(t) = h_0 \sqrt{\Omega_\Lambda + \Omega_m(1+z)^3}$ is the cosmic expansion rate following the Λ CDM model with the fractions of dark energy and matter density today, $\Omega_\Lambda = 0.685$ and $\Omega_m = 0.315$, respectively. The normalizing Hubble parameter is $h_0 = 67.3 \text{ km s}^{-1} \text{ Mpc}^{-1}$ [131]. Let's discuss the meaning of the terms on the r.h.s. of Eq. (24). In the first term, we have $\tilde{b}_i(t, E)$, which describes the energy loss due to redshift and other continuous processes. The second term, \mathcal{L}_i , corresponds to the luminosity density per co-moving volume of sources emitting particles i . The third term describes the annihilation of i -type particles through the interaction rate Γ_i , while the last term refers to the regeneration of particles i by an interaction of the form $j \rightarrow i$. Note that $E(z, \epsilon)$ is the solution of

$$\tilde{b}_i(z, E(z, \epsilon)) = -\frac{dE(z, \epsilon)}{dt} = -H(z)(1+z) \frac{dE(z, \epsilon)}{dz} = E(z, \epsilon)H(z) + b_i(z, E(z, \epsilon)), \quad (25)$$

with the initial condition $E(0, \epsilon) = \epsilon$, i.e. it is the energy that a particle i had at redshift z if it is observed at the Earth as having energy ϵ . To derive this identity, we have also used the relation $dt = -dz/((z+1)H(z))$. Note that the energy loss rate with time is written as a combination of $E(z, \epsilon)H(z)$, the energy loss due to redshift, and the rate of other continuous energy losses $b_i(z, E(z, \epsilon))$.

In order to solve the transport equation, we define

$$\tilde{n}_i(t, E) \equiv (1+z)n_i(t, E), \quad (26)$$

to re-write Eq. (24) as

$$\frac{d\tilde{n}_i(z, E)}{dz} = -\frac{1}{H(z)} \mathcal{L}_i^{\text{eff}}(z, E) - \frac{[\partial_E b_i(z, E) - \Gamma_i(z, E)]}{(z+1)H(z)} \tilde{n}_i(z, E), \quad (27)$$

so that

$$\tilde{n}_i(z, E) = \int_z^{z_{\text{max}}} dz \exp \left[\int_0^z \frac{\partial_E b_i(z', E(z', \epsilon)) - \Gamma_i(z', E(z', \epsilon))}{(z'+1)H(z')} dz' \right] \frac{1}{H(z)} \mathcal{L}_i^{\text{eff}}(z, E(z, \epsilon)), \quad (28)$$

where $\mathcal{L}_i^{\text{eff}}$ is defined as

$$\mathcal{L}_i^{\text{eff}}(z, E(z, \epsilon)) = \mathcal{L}_i(z, E(z, \epsilon)) + \sum_j \int dE' \frac{d\sigma_{ji}(E, E')}{dE} \frac{\tilde{n}_j(z, E')}{(1+z)}. \quad (29)$$

In our study $\mathcal{L}_i(z, E) = SE(z, m) \mathcal{L}_i(0, E)$ and $\mathcal{L}_i(0, E) \propto dN_p/dE_p$. The flux of particle i at Earth (per unit of area, solid angle and energy) is then

$$\phi_i(\epsilon) = \frac{1}{4\pi} \tilde{n}_i(0, E(0, \epsilon)). \quad (30)$$

B Neutrino-Ultralight Dark Matter Cross Section

For scalar dark matter, the interactions are given by

$$\mathcal{L} \supset -y_k \overline{\chi_R} \nu_{kL} S + y_k^* \overline{\nu}_{kL} \chi_R S^*, \quad (31)$$

where $i = 1, 2, 3$ represent mass indices. In order to compute the neutrino flux arriving at the Earth, we need to propagate the neutrino number density considering their interactions with dark matter. This is done by employing the transport equation (see Appendix A), where the depletion of n_i is governed by

$$\Gamma_i = \sum_{S'=S, \bar{S}} \sum_j n_{S'} \sigma_{iS' \rightarrow jS'}, \quad (32)$$

while the production of i neutrinos is described by

$$\frac{d\sigma_{ji}}{dE} = \sum_{S'=S, \bar{S}} n_{S'} \frac{d\sigma_{jS' \rightarrow iS'}}{dE}, \quad (33)$$

where E denotes the energy of the i -type neutrino.

The annihilation cross section is given by

$$\sigma_{iS(\bar{S}) \rightarrow jS(\bar{S})} = \frac{|y_i|^2 |y_j|^2}{64\pi s} \left\{ s \left(\frac{-s^2 + 5m_\chi^2 s - 2m_\chi^4}{(s - m_\chi^2)^2 (s + m_\chi^2)} \right) + 2 \log \left(\frac{s + m_\chi^2}{m_\chi^2} \right) \right\},$$

while the differential cross section for i -type neutrino creation can be written as

$$\frac{d\sigma_{jS(\bar{S}) \rightarrow iS(\bar{S})}}{dE_i} = -2m_S \frac{d\sigma_{jS(\bar{S}) \rightarrow iS(\bar{S})}}{dt} = \frac{m_S t |y_i|^2 |y_j|^2 (2m_\chi^4 - 2m_\chi^2(s+t) + s^2 + t^2)}{16\pi s (s - m_\chi^2)^2 (t - m_\chi^2)^2},$$

where s is the squared center-of-mass energy and $t = (p_S^{\text{ini}} - p_i)^2$.

References

- [1] **Super-Kamiokande** Collaboration, Y. Fukuda et al., *Evidence for oscillation of atmospheric neutrinos*, *Phys. Rev. Lett.* **81** (1998) 1562–1567, [[hep-ex/9807003](#)].
- [2] **IceCube** Collaboration, M. G. Aartsen et al., *Evidence for High-Energy Extraterrestrial Neutrinos at the IceCube Detector*, *Science* **342** (2013) 1242856, [[arXiv:1311.5238](#)].
- [3] V. S. Berezinsky and G. T. Zatsepin, *Cosmic neutrinos of superhigh energy*, *Yad. Fiz.* **11** (1970) 200–205.

- [4] F. W. Stecker, *Ultra-high energy photons, electrons and neutrinos, the microwave background, and the universal cosmic ray hypothesis*, *Astrophys. Space Sci.* **20** (1973) 47–57.
- [5] C. T. Hill and D. N. Schramm, *Ultra-high-Energy Cosmic Ray Neutrinos*, *Phys. Lett. B* **131** (1983) 247.
- [6] R. Alves Batista, R. M. de Almeida, B. Lago, and K. Kotera, *Cosmogenic photon and neutrino fluxes in the Auger era*, *JCAP* **01** (2019) 002, [[arXiv:1806.10879](#)].
- [7] **KM3NeT** Collaboration, S. Aiello et al., *Observation of an ultra-high-energy cosmic neutrino with KM3NeT*, *Nature* **638** (2025), no. 8050 376–382.
- [8] M. Ahlers and F. Halzen, *Minimal Cosmogenic Neutrinos*, *Phys. Rev. D* **86** (2012) 083010, [[arXiv:1208.4181](#)].
- [9] R. Aloisio, D. Boncioli, A. di Matteo, A. F. Grillo, S. Petrera, and F. Salamida, *Cosmogenic neutrinos and ultra-high energy cosmic ray models*, *JCAP* **10** (2015) 006, [[arXiv:1505.04020](#)].
- [10] M. Ackermann et al., *High-energy and ultra-high-energy neutrinos: A Snowmass white paper*, *JHEAp* **36** (2022) 55–110, [[arXiv:2203.08096](#)].
- [11] P. B. Denton and Y. Kini, *Ultra-High-Energy Tau Neutrino Cross Sections with GRAND and POEMMA*, *Phys. Rev. D* **102** (2020) 123019, [[arXiv:2007.10334](#)].
- [12] V. B. Valera, M. Bustamante, and C. Glaser, *The ultra-high-energy neutrino-nucleon cross section: measurement forecasts for an era of cosmic EeV-neutrino discovery*, *JHEP* **06** (2022) 105, [[arXiv:2204.04237](#)].
- [13] G.-y. Huang, S. Jana, M. Lindner, and W. Rodejohann, *Probing new physics at future tau neutrino telescopes*, *JCAP* **02** (2022), no. 02 038, [[arXiv:2112.09476](#)].
- [14] G.-y. Huang, S. Jana, M. Lindner, and W. Rodejohann, *Probing heavy sterile neutrinos at neutrino telescopes via the dipole portal*, *Phys. Lett. B* **840** (2023) 137842, [[arXiv:2204.10347](#)].
- [15] A. Garcia Soto, D. Garg, M. H. Reno, and C. A. Argüelles, *Probing quantum gravity with elastic interactions of ultrahigh-energy neutrinos*, *Phys. Rev. D* **107** (2023), no. 3 033009, [[arXiv:2209.06282](#)].
- [16] R. Heighton, L. Heurtier, and M. Spannowsky, *Hunting for neutral leptons with ultrahigh-energy neutrinos*, *Phys. Rev. D* **108** (2023), no. 5 055009, [[arXiv:2303.11352](#)].
- [17] M. Kirk, S. Okawa, and K. Wu, *A ν window onto leptoquarks?*, *JHEP* **12** (2023) 093, [[arXiv:2307.11152](#)].
- [18] **ANITA** Collaboration, R. Prechelt et al., *Analysis of a tau neutrino origin for the near-horizon air shower events observed by the fourth flight of the Antarctic Impulsive Transient Antenna*, *Phys. Rev. D* **105** (2022), no. 4 042001, [[arXiv:2112.07069](#)].
- [19] **ARA** Collaboration, P. Allison et al., *Constraints on the diffuse flux of ultrahigh energy neutrinos from four years of Askaryan Radio Array data in two stations*, *Phys. Rev. D* **102** (2020), no. 4 043021, [[arXiv:1912.00987](#)].
- [20] **ARIANNA** Collaboration, A. Anker et al., *Targeting ultra-high energy neutrinos with the ARIANNA experiment*, *Adv. Space Res.* **64** (2019) 2595–2609, [[arXiv:1903.01609](#)].
- [21] **GRAND** Collaboration, J. Álvarez-Muñiz et al., *The Giant Radio Array for Neutrino Detection (GRAND): Science and Design*, *Sci. China Phys. Mech. Astron.* **63** (2020), no. 1 219501, [[arXiv:1810.09994](#)].
- [22] **IceCube-Gen2** Collaboration, R. Abbasi et al., *Sensitivity studies for the IceCube-Gen2 radio array*, *PoS ICRC2021* (2021) 1183, [[arXiv:2107.08910](#)].

- [23] **POEMMA** Collaboration, A. V. Olinto et al., *The POEMMA (Probe of Extreme Multi-Messenger Astrophysics) observatory*, *JCAP* **06** (2021) 007, [[arXiv:2012.07945](#)].
- [24] **IceCube-Gen2** Collaboration, M. G. Aartsen et al., *IceCube-Gen2: the window to the extreme Universe*, *J. Phys. G* **48** (2021), no. 6 060501, [[arXiv:2008.04323](#)].
- [25] A. Connolly, R. S. Thorne, and D. Waters, *Calculation of High Energy Neutrino-Nucleon Cross Sections and Uncertainties Using the MSTW Parton Distribution Functions and Implications for Future Experiments*, *Phys. Rev. D* **83** (2011) 113009, [[arXiv:1102.0691](#)].
- [26] C. A. Argüelles, F. Halzen, L. Wille, M. Kroll, and M. H. Reno, *High-energy behavior of photon, neutrino, and proton cross sections*, *Phys. Rev. D* **92** (2015), no. 7 074040, [[arXiv:1504.06639](#)].
- [27] A. Garcia, R. Gauld, A. Heijboer, and J. Rojo, *Complete predictions for high-energy neutrino propagation in matter*, *JCAP* **09** (2020) 025, [[arXiv:2004.04756](#)].
- [28] R. Plestid and B. Zhou, *Final state radiation from high and ultrahigh energy neutrino interactions*, [arXiv:2403.07984](#).
- [29] **Pierre Auger** Collaboration, A. Abdul Halim et al., *Inference of the Mass Composition of Cosmic Rays with Energies from 1018.5 to 1020 eV Using the Pierre Auger Observatory and Deep Learning*, *Phys. Rev. Lett.* **134** (2025), no. 2 021001, [[arXiv:2406.06315](#)].
- [30] **Telescope Array** Collaboration, R. U. Abbasi et al., *Mass composition of ultrahigh energy cosmic rays from distribution of their arrival directions with the Telescope Array*, *Phys. Rev. D* **110** (2024), no. 2 022006, [[arXiv:2406.19286](#)].
- [31] A. Romero-Wolf and M. Ave, *Bayesian Inference Constraints on Astrophysical Production of Ultra-high Energy Cosmic Rays and Cosmogenic Neutrino Flux Predictions*, *JCAP* **07** (2018) 025, [[arXiv:1712.07290](#)].
- [32] J. Heinze, A. Fedynitch, D. Boncioli, and W. Winter, *A new view on Auger data and cosmogenic neutrinos in light of different nuclear disintegration and air-shower models*, *Astrophys. J.* **873** (2019), no. 1 88, [[arXiv:1901.03338](#)].
- [33] M. Ahlers, P. Denton, and M. Rameez, *Analyzing UHECR arrival directions through the Galactic magnetic field in view of the local universe as seen in 2MRS*, *PoS ICRC2017* (2017) 282.
- [34] **Pierre Auger** Collaboration, A. A. Halim et al., *Constraining the sources of ultra-high-energy cosmic rays across and above the ankle with the spectrum and composition data measured at the Pierre Auger Observatory*, *JCAP* **05** (2023) 024, [[arXiv:2211.02857](#)].
- [35] **Telescope Array** Collaboration, R. U. Abbasi et al., *Isotropy of Cosmic Rays beyond 1020 eV Favors Their Heavy Mass Composition*, *Phys. Rev. Lett.* **133** (2024), no. 4 041001, [[arXiv:2406.19287](#)].
- [36] K. Møller, P. B. Denton, and I. Tamborra, *Cosmogenic Neutrinos Through the GRAND Lens Unveil the Nature of Cosmic Accelerators*, *JCAP* **05** (2019) 047, [[arXiv:1809.04866](#)].
- [37] A. van Vliet, R. Alves Batista, and J. R. Hörandel, *Determining the fraction of cosmic-ray protons at ultrahigh energies with cosmogenic neutrinos*, *Phys. Rev. D* **100** (2019), no. 2 021302, [[arXiv:1901.01899](#)].
- [38] H. Yuksel, M. D. Kistler, J. F. Beacom, and A. M. Hopkins, *Revealing the High-Redshift Star Formation Rate with Gamma-Ray Bursts*, *Astrophys. J. Lett.* **683** (2008) L5–L8, [[arXiv:0804.4008](#)].

- [39] A. Caccianiga, T. Maccacaro, A. Wolter, R. Della Ceca, and I. M. Gioia, *On the cosmological evolution of bl lacs*, *Astrophys. J.* **566** (2002) 181, [[astro-ph/0110334](#)].
- [40] M. Ajello et al., *The Cosmic Evolution of Fermi BL Lacertae Objects*, *Astrophys. J.* **780** (2014) 73, [[arXiv:1310.0006](#)].
- [41] R. Alves Batista, A. Dundovic, M. Erdmann, K.-H. Kampert, D. Kuempel, G. Müller, G. Sigl, A. van Vliet, D. Walz, and T. Winchen, *CRPropa 3 - a Public Astrophysical Simulation Framework for Propagating Extraterrestrial Ultra-High Energy Particles*, *JCAP* **05** (2016) 038, [[arXiv:1603.07142](#)].
- [42] D. Wittkowski and K.-H. Kampert, *On the flux of high-energy cosmogenic neutrinos and the influence of the extragalactic magnetic field*, *Mon. Not. Roy. Astron. Soc.* **488** (2019), no. 1 L119–L122, [[arXiv:1810.03769](#)].
- [43] R. C. Gilmore, R. S. Somerville, J. R. Primack, and A. Domínguez, *Semi-analytic modelling of the extragalactic background light and consequences for extragalactic gamma-ray spectra*, *MNRAS* **422** (June, 2012) 3189–3207, [[arXiv:1104.0671](#)].
- [44] R. Alves Batista, D. Boncioli, A. di Matteo, and A. van Vliet, *Secondary neutrino and gamma-ray fluxes from SimProp and CRPropa*, *JCAP* **05** (2019) 006, [[arXiv:1901.01244](#)].
- [45] **Pierre Auger** Collaboration, A. Aab et al., *Measurement of the cosmic-ray energy spectrum above 2.5×10^{18} eV using the Pierre Auger Observatory*, *Phys. Rev. D* **102** (2020), no. 6 062005, [[arXiv:2008.06486](#)].
- [46] F. Fenu, *The cosmic ray energy spectrum measured with the pierre auger observatory*, *Advances in Space Research* **72** (2023), no. 8 3531–3537.
- [47] M. Sajjad Athar et al., *Status and perspectives of neutrino physics*, *Prog. Part. Nucl. Phys.* **124** (2022) 103947, [[arXiv:2111.07586](#)].
- [48] R. Gandhi, C. Quigg, M. H. Reno, and I. Sarcevic, *Neutrino interactions at ultrahigh-energies*, *Phys. Rev. D* **58** (1998) 093009, [[hep-ph/9807264](#)].
- [49] G. A. Askaryan, *Excess negative charge of an electron-photon shower and its coherent radio emission*, *Sov. Phys. JETP* **14** (1962) 441.
- [50] G. A. Askaryan, *Coherent Radio Emission from Cosmic Showers in Air and in Dense Media*, *Sov. Phys. JETP* **48** (1965) 988.
- [51] F. Testagrossa, D. F. G. Fiorillo, and M. Bustamante, *Two-detector flavor sensitivity to ultrahigh-energy cosmic neutrinos*, *Phys. Rev. D* **110** (2024), no. 8 083026, [[arXiv:2310.12215](#)].
- [52] J. F. Beacom, N. F. Bell, and S. Dodelson, *Neutrinoless universe*, *Phys. Rev. Lett.* **93** (2004) 121302, [[astro-ph/0404585](#)].
- [53] D. F. G. Fiorillo, G. Miele, S. Morisi, and N. Saviano, *Cosmogenic neutrino fluxes under the effect of active-sterile secret interactions*, *Phys. Rev. D* **101** (2020), no. 8 083024, [[arXiv:2002.10125](#)].
- [54] K. Blum, A. Hook, and K. Murase, *High energy neutrino telescopes as a probe of the neutrino mass mechanism*, [arXiv:1408.3799](#).
- [55] J. M. Berryman, A. De Gouvêa, K. J. Kelly, and Y. Zhang, *Lepton-Number-Charged Scalars and Neutrino Beamstrahlung*, *Phys. Rev. D* **97** (2018), no. 7 075030, [[arXiv:1802.00009](#)].
- [56] K. J. Kelly, M. Sen, W. Tangarife, and Y. Zhang, *Origin of sterile neutrino dark matter via secret neutrino interactions with vector bosons*, *Phys. Rev. D* **101** (2020), no. 11 115031, [[arXiv:2005.03681](#)].

- [57] J. M. Berryman et al., *Neutrino self-interactions: A white paper*, *Phys. Dark Univ.* **42** (2023) 101267, [[arXiv:2203.01955](#)].
- [58] I. R. Wang, X.-J. Xu, and B. Zhou, *Widen the Resonance: Probing a New Regime of Neutrino Self-Interactions with Astrophysical Neutrinos*, [arXiv:2501.07624](#).
- [59] N. Blinov, K. J. Kelly, G. Z. Krnjaic, and S. D. McDermott, *Constraining the Self-Interacting Neutrino Interpretation of the Hubble Tension*, *Phys. Rev. Lett.* **123** (2019), no. 19 191102, [[arXiv:1905.02727](#)].
- [60] E. Di Valentino, S. Gariazzo, and O. Mena, *Neutrinos in Cosmology*, [arXiv:2404.19322](#).
- [61] I. Esteban, S. Pandey, V. Brdar, and J. F. Beacom, *Probing secret interactions of astrophysical neutrinos in the high-statistics era*, *Phys. Rev. D* **104** (2021), no. 12 123014, [[arXiv:2107.13568](#)].
- [62] K. C. Y. Ng and J. F. Beacom, *Cosmic neutrino cascades from secret neutrino interactions*, *Phys. Rev. D* **90** (2014), no. 6 065035, [[arXiv:1404.2288](#)]. [Erratum: *Phys.Rev.D* 90, 089904 (2014)].
- [63] C. Creque-Sarbinowski, J. Hyde, and M. Kamionkowski, *Resonant neutrino self-interactions*, *Phys. Rev. D* **103** (2021), no. 2 023527, [[arXiv:2005.05332](#)].
- [64] L. Wolfenstein, *Different Varieties of Massive Dirac Neutrinos*, *Nucl. Phys. B* **186** (1981) 147–152.
- [65] S. T. Petcov, *On Pseudodirac Neutrinos, Neutrino Oscillations and Neutrinoless Double beta Decay*, *Phys. Lett. B* **110** (1982) 245–249.
- [66] J. W. F. Valle and M. Singer, *Lepton Number Violation With Quasi Dirac Neutrinos*, *Phys. Rev. D* **28** (1983) 540.
- [67] R. Kallosh, A. D. Linde, D. A. Linde, and L. Susskind, *Gravity and global symmetries*, *Phys. Rev. D* **52** (1995) 912–935, [[hep-th/9502069](#)].
- [68] D. Chang and O. C. W. Kong, *Pseudo-Dirac neutrinos*, *Phys. Lett. B* **477** (2000) 416–423, [[hep-ph/9912268](#)].
- [69] A. S. Joshipura and S. D. Rindani, *Phenomenology of pseudoDirac neutrinos*, *Phys. Lett. B* **494** (2000) 114–123, [[hep-ph/0007334](#)].
- [70] M. Lindner, T. Ohlsson, and G. Seidl, *Seesaw mechanisms for Dirac and Majorana neutrino masses*, *Phys. Rev. D* **65** (2002) 053014, [[hep-ph/0109264](#)].
- [71] V. Berezinsky, M. Narayan, and F. Vissani, *Mirror model for sterile neutrinos*, *Nucl. Phys. B* **658** (2003) 254–280, [[hep-ph/0210204](#)].
- [72] E. Ma and R. Srivastava, *Dirac or inverse seesaw neutrino masses with $B - L$ gauge symmetry and S_3 flavor symmetry*, *Phys. Lett. B* **741** (2015) 217–222, [[arXiv:1411.5042](#)].
- [73] J. W. F. Valle and C. A. Vaquera-Araujo, *Dynamical seesaw mechanism for Dirac neutrinos*, *Phys. Lett. B* **755** (2016) 363–366, [[arXiv:1601.05237](#)].
- [74] Y. H. Ahn, S. K. Kang, and C. S. Kim, *A Model for Pseudo-Dirac Neutrinos: Leptogenesis and Ultra-High Energy Neutrinos*, *JHEP* **10** (2016) 092, [[arXiv:1602.05276](#)].
- [75] K. S. Babu, X.-G. He, M. Su, and A. Thapa, *Naturally light Dirac and pseudo-Dirac neutrinos from left-right symmetry*, *JHEP* **08** (2022) 140, [[arXiv:2205.09127](#)].
- [76] M. Kobayashi and C. S. Lim, *Pseudo Dirac scenario for neutrino oscillations*, *Phys. Rev. D* **64** (2001) 013003, [[hep-ph/0012266](#)].
- [77] I. Martinez-Soler, Y. F. Perez-Gonzalez, and M. Sen, *Signs of pseudo-Dirac neutrinos in SN1987A data*, *Phys. Rev. D* **105** (2022), no. 9 095019, [[arXiv:2105.12736](#)].

- [78] J. Franklin, Y. F. Perez-Gonzalez, and J. Turner, *JUNO as a probe of the pseudo-Dirac nature using solar neutrinos*, *Phys. Rev. D* **108** (2023), no. 3 035010, [[arXiv:2304.05418](#)].
- [79] K. Carloni, I. Martínez-Soler, C. A. Argüelles, K. S. Babu, and P. S. B. Dev, *Probing pseudo-Dirac neutrinos with astrophysical sources at IceCube*, *Phys. Rev. D* **109** (2024) L051702, [[arXiv:2212.00737](#)].
- [80] P. S. B. Dev, P. A. N. Machado, and I. Martínez-Soler, *Pseudo-Dirac Neutrinos and Relic Neutrino Matter Effect on the High-energy Neutrino Flavor Composition*, [arXiv:2406.18507](#).
- [81] I. Esteban, M. C. Gonzalez-Garcia, M. Maltoni, I. Martínez-Soler, J. a. P. Pinheiro, and T. Schwetz, *NuFit-6.0: Updated global analysis of three-flavor neutrino oscillations*, [arXiv:2410.05380](#).
- [82] V. Brdar, J. Kopp, J. Liu, P. Prass, and X.-P. Wang, *Fuzzy dark matter and nonstandard neutrino interactions*, *Phys. Rev. D* **97** (2018), no. 4 043001, [[arXiv:1705.09455](#)].
- [83] L. F. Abbott and P. Sikivie, *A Cosmological Bound on the Invisible Axion*, *Phys. Lett. B* **120** (1983) 133–136.
- [84] M. Dine and W. Fischler, *The Not So Harmless Axion*, *Phys. Lett. B* **120** (1983) 137–141.
- [85] J. Preskill, M. B. Wise, and F. Wilczek, *Cosmology of the Invisible Axion*, *Phys. Lett. B* **120** (1983) 127–132.
- [86] E. J. Chun, *Neutrino Transition in Dark Matter*, [arXiv:2112.05057](#).
- [87] A. Berlin, *Neutrino Oscillations as a Probe of Light Scalar Dark Matter*, *Phys. Rev. Lett.* **117** (2016), no. 23 231801, [[arXiv:1608.01307](#)].
- [88] G. Krnjaic, P. A. N. Machado, and L. Necib, *Distorted neutrino oscillations from time varying cosmic fields*, *Phys. Rev. D* **97** (2018), no. 7 075017, [[arXiv:1705.06740](#)].
- [89] F. Capozzi, I. M. Shoemaker, and L. Vecchi, *Neutrino Oscillations in Dark Backgrounds*, *JCAP* **07** (2018) 004, [[arXiv:1804.05117](#)].
- [90] A. Dev, P. A. N. Machado, and P. Martínez-Miravé, *Signatures of ultralight dark matter in neutrino oscillation experiments*, *JHEP* **01** (2021) 094, [[arXiv:2007.03590](#)].
- [91] M. Losada, Y. Nir, G. Perez, and Y. Shpilman, *Probing scalar dark matter oscillations with neutrino oscillations*, *JHEP* **04** (2022) 030, [[arXiv:2107.10865](#)].
- [92] A. Dev, G. Krnjaic, P. Machado, and H. Ramani, *Constraining feeble neutrino interactions with ultralight dark matter*, *Phys. Rev. D* **107** (2023), no. 3 035006, [[arXiv:2205.06821](#)].
- [93] H. Davoudiasl and P. B. Denton, *Sterile neutrino shape shifting caused by dark matter*, *Phys. Rev. D* **108** (2023), no. 3 035013, [[arXiv:2301.09651](#)].
- [94] T. Gherghetta and A. Shkerin, *Probing a local dark matter halo with neutrino oscillations*, *Phys. Rev. D* **108** (2023), no. 9 095009, [[arXiv:2305.06441](#)].
- [95] M. Sen and A. Y. Smirnov, *Refractive neutrino masses, ultralight dark matter and cosmology*, *JCAP* **01** (2024) 040, [[arXiv:2306.15718](#)].
- [96] **Kamiokande-II** Collaboration, K. Hirata et al., *Observation of a Neutrino Burst from the Supernova SN 1987a*, *Phys. Rev. Lett.* **58** (1987) 1490–1493.
- [97] K. S. Hirata et al., *Observation in the Kamiokande-II Detector of the Neutrino Burst from Supernova SN 1987a*, *Phys. Rev. D* **38** (1988) 448–458.
- [98] R. M. Bionta et al., *Observation of a Neutrino Burst in Coincidence with Supernova SN 1987a in the Large Magellanic Cloud*, *Phys. Rev. Lett.* **58** (1987) 1494.

- [99] E. N. Alekseev, L. N. Alekseeva, I. V. Krivosheina, and V. I. Volchenko, *Detection of the Neutrino Signal From SN1987A in the LMC Using the Inr Baksan Underground Scintillation Telescope*, *Phys. Lett. B* **205** (1988) 209–214.
- [100] **IceCube**, **Fermi-LAT**, **MAGIC**, **AGILE**, **ASAS-SN**, **HAWC**, **H.E.S.S.**, **INTEGRAL**, **Kanata**, **Kiso**, **Kapteyn**, **Liverpool Telescope**, **Subaru**, **Swift NuSTAR**, **VERITAS**, **VLA/17B-403** Collaboration, M. G. Aartsen et al., *Multimessenger observations of a flaring blazar coincident with high-energy neutrino IceCube-170922A*, *Science* **361** (2018), no. 6398 eaat1378, [[arXiv:1807.08816](#)].
- [101] B. Bertoni, S. Ipek, D. McKeen, and A. E. Nelson, *Constraints and consequences of reducing small scale structure via large dark matter-neutrino interactions*, *JHEP* **04** (2015) 170, [[arXiv:1412.3113](#)].
- [102] R. J. Wilkinson, C. Boehm, and J. Lesgourgues, *Constraining Dark Matter-Neutrino Interactions using the CMB and Large-Scale Structure*, *JCAP* **05** (2014) 011, [[arXiv:1401.7597](#)].
- [103] M. Escudero, L. Lopez-Honorez, O. Mena, S. Palomares-Ruiz, and P. Villanueva-Domingo, *A fresh look into the interacting dark matter scenario*, *JCAP* **06** (2018) 007, [[arXiv:1803.08427](#)].
- [104] P. Brax, C. van de Bruck, E. Di Valentino, W. Giarè, and S. Trojanowski, *Extended analysis of neutrino-dark matter interactions with small-scale CMB experiments*, *Phys. Dark Univ.* **42** (2023) 101321, [[arXiv:2305.01383](#)].
- [105] K. Murase, *High energy neutrino early afterglows gamma-ray bursts revisited*, *Phys. Rev. D* **76** (2007) 123001, [[arXiv:0707.1140](#)].
- [106] K. Fang and K. Murase, *Linking High-Energy Cosmic Particles by Black Hole Jets Embedded in Large-Scale Structures*, *Nature Phys.* **14** (2018), no. 4 396–398, [[arXiv:1704.00015](#)].
- [107] G. F. S. Alves, M. Hostert, and M. Pospelov, *Neutron portal to ultra-high-energy neutrinos*, [arXiv:2503.14419](#).
- [108] C. Righi, A. Palladino, F. Tavecchio, and F. Vissani, *EeV astrophysical neutrinos from flat spectrum radio quasars*, *Astron. Astrophys.* **642** (2020) A92, [[arXiv:2003.08701](#)].
- [109] X. Rodrigues, J. Heinze, A. Palladino, A. van Vliet, and W. Winter, *Active Galactic Nuclei Jets as the Origin of Ultrahigh-Energy Cosmic Rays and Perspectives for the Detection of Astrophysical Source Neutrinos at EeV Energies*, *Phys. Rev. Lett.* **126** (2021), no. 19 191101, [[arXiv:2003.08392](#)].
- [110] **IceCube** Collaboration, R. Abbasi et al., *A search for extremely-high-energy neutrinos and first constraints on the ultra-high-energy cosmic-ray proton fraction with IceCube*, [arXiv:2502.01963](#).
- [111] S. W. Li, P. Machado, D. Naredo-Tuero, and T. Schwemberger, *Clash of the Titans: ultra-high energy KM3NeT event versus IceCube data*, [arXiv:2502.04508](#).
- [112] **IceCube** Collaboration, M. G. Aartsen et al., *Differential limit on the extremely-high-energy cosmic neutrino flux in the presence of astrophysical background from nine years of IceCube data*, *Phys. Rev. D* **98** (2018), no. 6 062003, [[arXiv:1807.01820](#)].
- [113] P. S. Pasquini and O. L. G. Peres, *Bounds on Neutrino-Scalar Yukawa Coupling*, *Phys. Rev. D* **93** (2016), no. 5 053007, [[arXiv:1511.01811](#)]. [Erratum: *Phys.Rev.D* **93**, 079902 (2016)].
- [114] A. de Gouvêa, P. S. B. Dev, B. Dutta, T. Ghosh, T. Han, and Y. Zhang, *Leptonic Scalars at the LHC*, *JHEP* **07** (2020) 142, [[arXiv:1910.01132](#)].

- [115] A. P. Lessa and O. L. G. Peres, *Revising limits on neutrino-Majoron couplings*, *Phys. Rev. D* **75** (2007) 094001, [[hep-ph/0701068](#)].
- [116] **KamLAND-Zen** Collaboration, A. Gando et al., *Limits on Majoron-emitting double-beta decays of Xe-136 in the KamLAND-Zen experiment*, *Phys. Rev. C* **86** (2012) 021601, [[arXiv:1205.6372](#)].
- [117] S. A. Kharusi et al., *Search for Majoron-emitting modes of ^{136}Xe double beta decay with the complete EXO-200 dataset*, *Phys. Rev. D* **104** (2021), no. 11 112002, [[arXiv:2109.01327](#)].
- [118] K. Blum, Y. Nir, and M. Shavit, *Neutrinoless double-beta decay with massive scalar emission*, *Phys. Lett. B* **785** (2018) 354–361, [[arXiv:1802.08019](#)].
- [119] Y. Farzan, M. Lindner, W. Rodejohann, and X.-J. Xu, *Probing neutrino coupling to a light scalar with coherent neutrino scattering*, *JHEP* **05** (2018) 066, [[arXiv:1802.05171](#)].
- [120] M. Atzori Corona, M. Cadeddu, N. Cargioli, F. Dordei, C. Giunti, Y. F. Li, E. Picciau, C. A. Ternes, and Y. Y. Zhang, *Probing light mediators and $(g - 2)_\mu$ through detection of coherent elastic neutrino nucleus scattering at COHERENT*, *JHEP* **05** (2022) 109, [[arXiv:2202.11002](#)].
- [121] L. Heurtier and Y. Zhang, *Supernova Constraints on Massive (Pseudo)Scalar Coupling to Neutrinos*, *JCAP* **02** (2017) 042, [[arXiv:1609.05882](#)].
- [122] G.-y. Huang, T. Ohlsson, and S. Zhou, *Observational Constraints on Secret Neutrino Interactions from Big Bang Nucleosynthesis*, *Phys. Rev. D* **97** (2018), no. 7 075009, [[arXiv:1712.04792](#)].
- [123] C. D. Kreisch, F.-Y. Cyr-Racine, and O. Doré, *Neutrino puzzle: Anomalies, interactions, and cosmological tensions*, *Physical Review D* **101** (June, 2020).
- [124] A. Poudou, T. Simon, T. Montandon, E. M. Teixeira, and V. Poulin, *Self-interacting neutrinos in light of recent CMB and LSS data*, [arXiv:2503.10485](#).
- [125] Z. Chen, J. Liao, J. Ling, and B. Yue, *Constraining super-light sterile neutrinos at Borexino and KamLAND*, *JHEP* **09** (2022) 004, [[arXiv:2205.07574](#)].
- [126] S. Ansarifard and Y. Farzan, *Revisiting pseudo-Dirac neutrino scenario after recent solar neutrino data*, *Phys. Rev. D* **107** (2023), no. 7 075029, [[arXiv:2211.09105](#)].
- [127] J. F. Beacom, N. F. Bell, D. Hooper, J. G. Learned, S. Pakvasa, and T. J. Weiler, *PseudoDirac neutrinos: A Challenge for neutrino telescopes*, *Phys. Rev. Lett.* **92** (2004) 011101, [[hep-ph/0307151](#)].
- [128] T. Rink and M. Sen, *Constraints on pseudo-Dirac neutrinos using high-energy neutrinos from NGC 1068*, *Phys. Lett. B* **851** (2024) 138558, [[arXiv:2211.16520](#)].
- [129] K. Dixit, L. S. Miranda, and S. Razzaque, *Searching for Pseudo-Dirac neutrinos from Astrophysical sources in IceCube data*, [arXiv:2406.06476](#).
- [130] M. Ahlers, L. A. Anchordoqui, and S. Sarkar, *Neutrino diagnostics of ultra-high energy cosmic ray protons*, *Phys. Rev. D* **79** (2009) 083009, [[arXiv:0902.3993](#)].
- [131] **Planck** Collaboration, N. Aghanim et al., *Planck 2018 results. VI. Cosmological parameters*, *Astron. Astrophys.* **641** (2020) A6, [[arXiv:1807.06209](#)]. [Erratum: *Astron.Astrophys.* 652, C4 (2021)].